Received: 11 April 2023 | Revised: 19 June 2023 | Accepted: 21 June 2023

DOI: 10.1002/rpm.20230005

REVIEW ARTICLE

RESPONSIVE MATERIALS Open Access WILEY

Circularly polarized luminescence in chiral orientationally ordered soft matter systems

Jiao Liu[1] | **Zhen-Peng Song**[1] | **Lu-Yao Sun**[1] | **Bing-Xiang Li**[1] | **Yan-Qing Lu**[2] | **Quan Li**[3]

[1]College of Electronic and Optical Engineering & College of Flexible Electronics (Future Technology), Nanjing University of Posts and Telecommunications, Nanjing, China

[2]National Laboratory of Solid State Microstructures & Collaborative Innovation Center of Advanced Microstructures & College of Engineering and Applied Sciences, Nanjing University, Nanjing, China

[3]Institute of Advanced Materials & School of Chemistry and Chemical Engineering, Southeast University, Nanjing, China

Correspondence

Bing-Xiang Li, Yan-Qing Lu, and Quan Li.
Email: bxli@njupt.edu.cn, yqlu@nju.edu.cn, and quanli3273@gmail.com

Abstract

Circularly polarized luminescent (CPL) materials have received significant attention in the field of fundamental science recently. These materials offer substantial advancement of technological applications, such as optical data storage, displays, and quantum communication. Various strategies have been proposed in self-assembled materials consisting of inorganic, organic, and hybrid systems, particularly in the chiral orientationally ordered soft matter systems (e.g., chiral liquid crystals (LCs) and LC polymers). However, developing scientific approaches to achieve the pronounced and steerable circularly polarized light emission remains challenging. Herein, we present a comprehensive review on the recent development of CPL materials based on chiral LCs, including thermotropic LCs (cholesteric LCs and bent-core LCs), lyotropic LCs (nanocellulose LCs and polyacetylene-based LCs), and LC polymers (cholesteric LC-based polymers, helical nanofibers, and helical network). In addition, the fundamental mechanisms, design principles, and potential applications based on these chiral LCs and LC polymers in soft matter systems are systematically reviewed. This review summarizes with a prospect on the latent challenges, which can strengthen our understanding of the basic principles of CPL in chiral orientationally ordered soft matter systems and provide a new insight into the progress in several fields, such as chemistry, materials science, optics, electronics, and biology.

Keywords

bent-core liquid crystal, cellulose nanocrystal, chirality, cholesteric liquid crystal, circularly polarized luminescence, liquid crystal polymer

1 | INTRODUCTION

Chirality, first defined by Lord Kelvin,[1] refers to the geometrically symmetric property of an object or molecule, which cannot overlap with its mirror image through any translation or rotation,[2–5] and is inextricably linked to that of enantiomers.[6,7] Chirality, being an intriguing characteristic of molecules, objects, and materials, has received significant attention of scientists.[8] Chiral materials are ubiquitous in multidisciplinary fields,[9–11] such as chemistry, physiology, medicine, materials science, and physics from atomic, macroscopic, to galactic scales.[12] In chemistry, various two-dimensional (2D) and three-dimensional (3D) chiral mechanical metamaterials are synthesized with outstanding mechanical and physical properties, which are not available in nature.[13] In physiological processes, nature favors one type

Jiao Liu, Zhen-Peng Song, and Lu-Yao Sun contributed equally to this work.

of chirality, thereby selecting *L*-amino acids as the primary constituents of proteins and *D*-sugars as the major parts of deoxyribonucleic acid (DNA) and ribonucleic acid.[14] This is called "homochirality," which indicates that the physiological processes demonstrate distinct stereoselectivity, although exceptions do exist. The chiral biomolecules, such as nucleic acids and amino acids, are viewed as fundamental elements of life and critical components in biological systems.[14,15] In addition, chirality is observed in plants and animals. For example, the *Convolvulus arvensis* demonstrates a right-handed growth, whereas the trumpet honeysuckle of the *Lonicera sempervirens* shows the growth of left handedness; the *Lymnaea peregra* snail shell presents right-handed spiral, whereas the *Laciniaria biplicata* shell is left-handed spiral.[16] Transferring the chirality from molecules to nanomaterials results in chiroptical effects in these chiral nanostructures and facilitates the chiral functional material in the applications of sensing, imaging, catalysis, and optics.[17,18] Over the past decades, the probability of transferring molecular chirality to sorts of plasmonic nanostructures[19] has been demonstrated for developing advanced chiral nanomaterials with an unprecedented chiroptical activity.[20] Chiral plasmonic nanostructures[18,21–23] have gained attention since Whetten and Schaaff[24] discovered the optical activity and confirmed the existence of nanoscale chirality in the glutathione nanoclusters. The important characteristic of the chiral nanostructures is their diverse responses to the right or left circularly polarized (CP) light, generating a remarkable optical activity based on the different refractive indices and circular polarized emissions.[25,26] Once CP light acts on the plasmonic nanostructures, the resonance is higher for one circular polarization than the other, referred to as chiral plasmonic effects.[27] The gold nanostructures are the most common chiral plasmonic nanomaterials, which utilize amino acids as structure-directing agents to control the chiral morphology.[28–30] Kotov et al.[31] embedded the chiral nanoparticles into the semiconductor helices to obtain controllable chiroptical activity and enantiomer selectivity. Wang et al.[32] realized the anisotropic gold nanorod helical superstructures and designed an arrangement in the "X" pattern, which resembles that of DNA. The high optical activity of chiral nanostructures is closely related to the plasmonic effects, multiscale chirality, and strongly polarizable components.[33]

Templates, such as DNA,[34-36] peptides,[37] and liquid crystals (LCs),[38] are used in chiral assemblies. In the orientationally ordered soft matter systems, the LCs, one of the most classical templates, are the intermediate phases between solid and isotropic fluid, which are conspicuous and intriguing state of matters with a long-range orientational order. They are generally classified into thermotropic and lyotropic LCs.[39] In addition, LCs based on polymers, gels, inorganic-based hybrids, and supramolecular complexes are widely considered as the emergingly promising matters that involve chemistry, optics, biotechnology, energy, and sensing.[40-43] The introduction of the molecular chirality into LCs gives rise to various chiral LC phases, for example, cholesteric,[44] chiral smectic (Smectic A*, Smectic C*),[16] and double-twist structure of blue phases (BPs)[45-49] with unprecedented properties.[29,50-55] Chiral nematic LCs can be achieved from cholesteric LCs or by doping chiral additives to nematic LCs. Among these LC phases, the cholesteric LCs exhibit attractive optical properties because of their self-organized helical superstructures with a one-dimensional (1D) orientational order that is considered as the observable scale molecular chirality. The CP light is selectively reflected when light propagates through the helical superstructures of cholesteric LCs.[56,57] In case of bent-core mesogens, the steric hindrance avoids the free rotations along the long bent-core molecular axis, resulting in ferro- or antiferroelectric LCs (SmCP and B2 phases).[58] The smectic layers in bent-core mesogens are intrinsically chiral in the presence of tilted molecules. Achiral molecules with bent-geometry contribute in identifying the helical nematic phase (N_{TB} phase) and B4 phase with a number of layered structures, exhibiting chiral morphologies. Chirality-related research in LCs is one of the most interesting subjects toward the field of material science.

Recently, CP luminescence (CPL) materials have gained significant concerns for developing photonic devices using advanced technologies, such as chiral sensing,[59-61] optical communication for spintronics,[62-64] optical data storage,[65,66] spin-optoelectronic circuits,[67] and organic optoelectronic devices.[68-70] Several CPL-active materials, which consist of organic molecules, lanthanide metal complexes, and chiral LCs, have been demonstrated with excellent optical and electronic properties.[71-76] The chiral molecules, achiral species, and inorganic nanoparticles can self-assemble into chiral nanoassemblies with considerable CPL activity. Among different chiral materials used for CPL, the LCs are capable of directing the functional building blocks of the nanoscale range by self-assembly into the high-ordered chiral nanomaterials. The nanoarchitectures of the chiral LCs broadly exist in living organisms; these nanoarchitectures widely known natural materials include dactyl clubs of the *Odontodactylus scyllarus*,[77] *Gonodactylus smithi*,[78] and *Pollia condensata* fruit.[79] The *Chrysina resplendens* with a metallic gold color originates from two helical layers. Kitson et al.[80] fabricated structures similar to these biological materials using a nematic alignment layer, one cholesteric LC layer with a specific reflection peak at 639 nm and the other cholesteric LC layer with a reflection peak at 562 nm. The obtained structure exhibited the golden color, which is similar to the color of beetles. *Chrysina gloriosa* is able to reflect left-handed circularly polarized light (LCP) but absorb right-handed circularly polarized light (RCP) since the cholesteric nanoarchitectures present in their exoskeletons.[81] The *Plusiotis batesi* with a helical structure demonstrates selective reflection. In contrast, the *Plusiotis resplendens* with an anisotropic layer exhibits the total reflection. Takezoe et al.[82] constructed an anisotropic layer structure with an optical heterojunction. This structure with a periodicity of the helix was inserted between

polymer-based cholesteric LC layers to fabricate the electrotunable optical diode, which was based on the photonic bandgap (PBG) of LC heterojunctions. The fruit of *P. condensata* with iridescent colors owing to the chiral gyroid photonic crystals[83] was explored to design the advanced chiral nanomaterials using LC-based nanoassemblies. In addition, the *chitin fibril* exhibits a characteristic helicoidal structure with periodic regions, where the helicoidal architectures dissipate energy by propagating microcracks. This provides valuable insights into the biological materials and encourages researchers to explore the CPL-based LCs in diverse applications.[39]

There have been many reviews related to CPL-active materials recently, but most of them concentrate on organic micro-/nanostructures with CPL activity (self-assembly of small molecules, self-assembly of micro-/nanoscale architectures, and self-assembly of π-conjugated polymers), luminescent LC materials (fluorescent materials, phosphorescent materials, and lanthanide complexes), and the emission properties in the context of linearly polarized electroluminescence, and the CPL only in chiral nematic LC systems.[84-86] However, the target of our review focuses on CPL in chiral orientationally ordered soft matter systems. The systems are chiral LCs, including thermotropic LCs (cholesteric LCs and bent-core LCs), lyotropic LCs (nanocellulose LCs and polyacetylene-based LCs), and LC polymers (cholesteric LC-based polymers, helical nanofibers, and helical network). Herein, we provide a comprehensive review on the CPL-active chiral LCs and LC polymers of soft matter systems (Figure 1). We primarily focus on the recent progresses and emphasize the appealing findings to amplify the CPL dissymmetry factor (g_{lum}) for providing an insight into the applied strategies for regulating CPL signals. The concept and generation of CPL are explained. In addition, the cholesteric LCs with the spatial helicoidal orientational superstructures owing to their tunable pitch and helix-twist handedness are discussed. Inducing CPL in these superstructures using inorganic and organic dopants, such as quantum dots (QDs), nanoparticles, metal nanocrystals, combination of polyacrylonitrile (PAN) and perovskites, upconversion nanoparticles (UNPs), chiral emitters, and light-driven molecular motors (MMs) is reviewed. The CPL can be observed in bent-core LCs with chiral additives. The chiral lyotropic LCs, such as cellulose and chiral disubstituted LC polyacetylene, acting as a 1D chiral photonic crystal, can tailor CPL due to their cholesteric structures. Moreover, the LC polymers exhibit potential applications with a large g_{lum} and high luminescent efficiency owing to the polymerization in chiral LC systems. Finally, we conclude the progresses of CPL-active chiral LCs and LC polymers in this emerging field to encourage scientists to develop more effective CPL-active materials in chemical and biological sensing, optical information processing, and organic light-emitting diodes (LEDs). This review is to strengthen the fundamental understanding of CPL-active LCs and to bring substantial advancement to the CPL-based devices as well as their potential in light emission applications, such as quantum communications, optical information processing, and photoelectric devices.

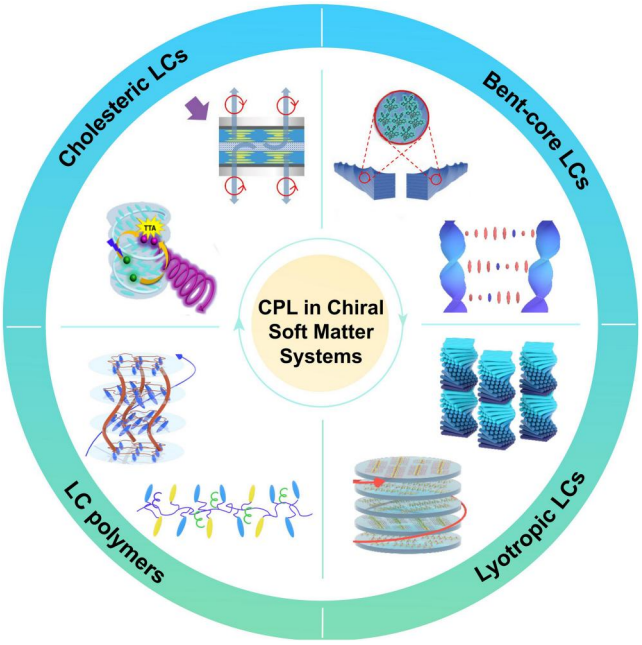

FIGURE 1 Representative chiral LCs with characteristics of CPL, including cholesteric LCs (Reproduced with permission.[87,88] Copyright 2019, Wiley-VCH and Copyright 2020, Springer Nature), bent-core LCs (Reproduced with permission.[89] Copyright 2022, American Chemical Society), lyotropic LCs (Reproduced with permission.[90] Copyright 2019 Wiley-VCH), and LC polymers (Reproduced with permission.[91,92] Copyright 2021 American Chemical Society). CPL, circularly polarized luminescence; LCs, liquid crystals.

2 | CONCEPT AND GENERATION OF CPL

Unpolarized light, such as natural and other common sources, is a mixture of two polarized streams, each with half of the intensity. Unpolarized light can be turned into the polarized light when one of these streams has higher power than the other. Polarized light can be divided into linearly, CP light, and elliptically polarized light depending on the difference in the direction of wave vectors, which is vertical to light propagation.[93] Among different types of the polarized light, the CP light is receiving significant interest owing to its latent applications in optical sensors, photoelectric devices, 3D displays, chiroptical materials, and controlling the supramolecular chirality.[60,62,65,67,94,95]

Traditionally, CP light is generated via a physical approach with a linear polarizer and a quarter-wave retarder. However, this method results in a significant loss of energy (at least 50% of the energy) during the transmission.[84,93] According to the CPL generation mechanism, a linear polarizer first converts the emitted unpolarized light into the linearly polarized light, then resolved into LCP or RCP light using a quarter-wave plate (Figure 2a). The CP light can

distinguish the absolute configuration and composition of enantiomers.[96] Additionally, the mechanism of electronic circular dichroism (CD) is founded on differential absorption of LCP and RCP light. In the CD spectrophotometer, LCP and RCP light are alternately produced using the xenon lamp, then they pass through a chiral sample (Figure 2b). The conformational changes of the secondary or tertiary structures of proteins and nucleic acids and their thermal stability can be assessed by CD-based techniques.[97] The CD spectrum signal is obtained by comparing the original and remanent light intensity with the cotton effect induced at the absorption position. This effect is utilized in emitting devices or light harvesting with emissivity or detectivity of CP light, respectively.[98] In contrast, the unpolarized excitation light is generally applied to remove the effect of the polarized light when detecting true CPL signals from the sample. The measurement is based on different emissions of LCP and RCP light, induced by chiral luminescent samples in the excited state. Thus, it is always accompanied with the emission spectrum.[86,93,99] The mechanism is illustrated in Figure 2c. Notably, CD signals in chiral luminescent systems are not necessarily required to observe the CPL. In general, the CPL-active materials demonstrate the characteristic of the cotton effect.

In the CPL-active materials, the major challenge is to obtain a large luminescent dissymmetry factor, g_{lum}, which is employed to quantify the level of CPL.

$$g_{lum} = 2 \times (I_L - I_R)/(I_L + I_R), \quad (1)$$

where I_L and I_R are intensities of the LCP and RCP emissions, respectively. The maximum value of $|g_{lum}|$ is 2, which

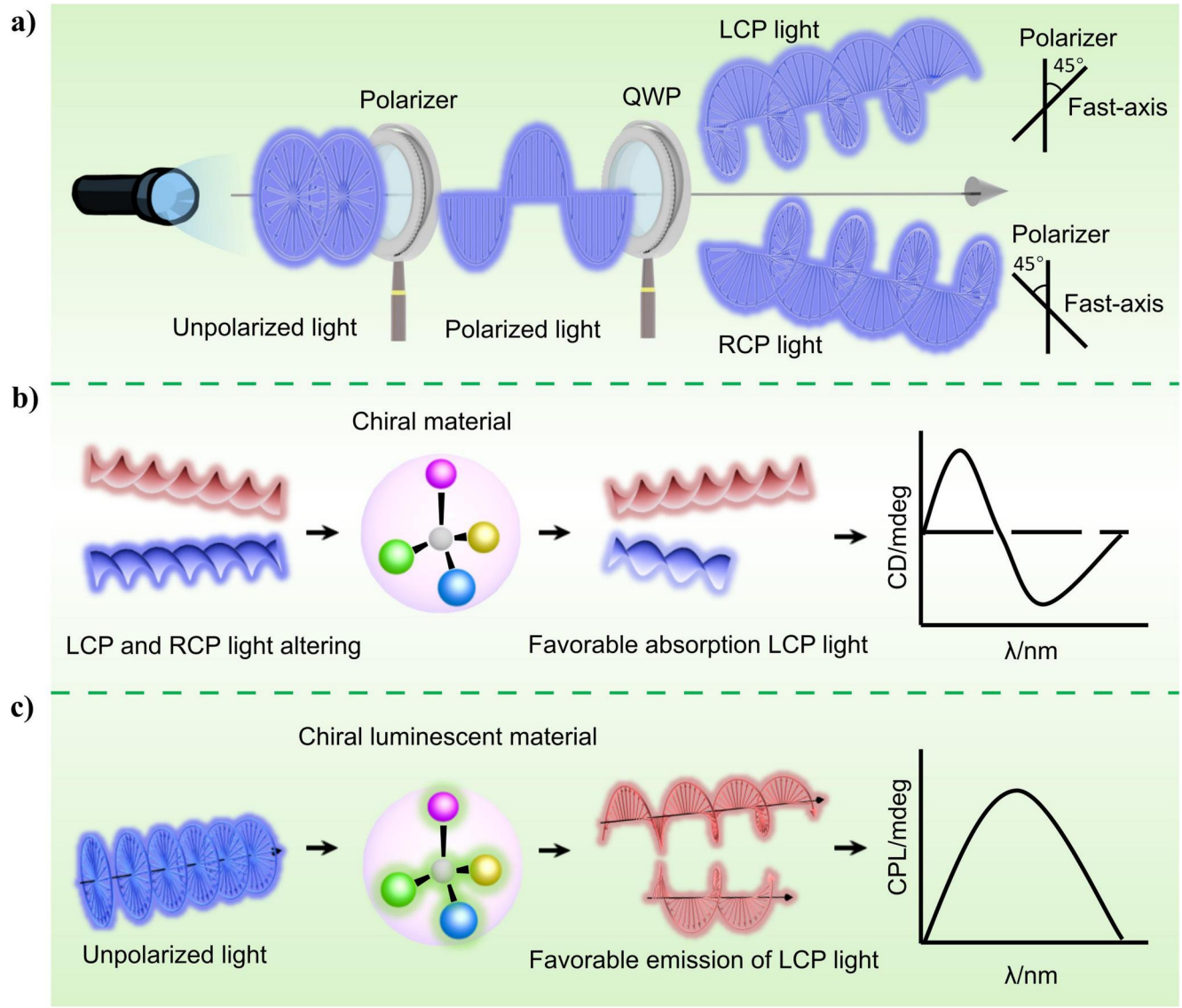

FIGURE 2 Schematic of (a) circular polarized light, (b) CD, and (c) CPL. CD, circular dichroism; CPL, circularly polarized luminescence.

means completely left or right CP light.[86] An efficient way to attain the CPL activity is to fabricate the chiral luminescent organic or inorganic materials. For example, connecting a chiral part with a luminophore component by covalent bond is a prevalent approach[93,100]; however, the synthesis process is inevitably long and sophisticated. Moreover, the inorganic CPL-active materials need relatively complicated synthesis processes with chiral reagents[101] using the expensive lithography techniques. Organic materials show the CPL activity by integrating chiral agents and luminescent moiety via hydrogen bonds,[102] transition metal complexes, conjugated polymers, and supramolecular assemblies.[103-105] Particularly, the bioimaging applications of phosphorescent heavy-metal complexes were systematically studied in the d^6, d^8, and d^{10} electronic configurations,[106,107] followed by the reversible tuning of the luminescent properties (i.e., emission intensity, lifetime, and wavelength under external stimuli such as solvent, temperature, electric and magnetic fields, and mechanical force).[108] However, they endure the low $|g_{lum}|$, thereby limiting the practical applications. Hence, an intriguing, versatile, and inexpensive approach by self-assembly for designing CPL-active materials gives a novel insight for achieving CPL-active materials. Owing to the property of self-assembly, the chiral molecules, achiral species, inorganic nanoparticles, and nanorods are able to be self-assembled into chiral nanoassemblies with considerable CPL activity.[8,36,69,109,110] Self-assembly is efficient in enhancing the g_{lum} in plasmon resonance, such as Förster resonance energy transfer,[111,112] and triplet-triplet-annihilation photon upconversion,[113] and LCs.[20] For applications, a higher $|g_{lum}|$ value suggests that the emitted light has a better polarization degree, which corresponds to the lower energy loss. Three approaches, namely achiral luminescent molecules, chiral luminescent molecules assembly, and chirality transfer between chiral molecules, are generally used to achieve CPL in supramolecular assemblies.[93] CPL primarily derives from the selective reflection of cholesteric LCs.[114] In addition, the CPL can be generated from the chiral superstructures, formed by the helical nanofilaments embedded with rod-like molecules or additives. Generally, the guidance of polarized light is valuable in several advanced technology applications, containing nonlinear optics, LC displays, optical storage devices, light-emitting transistors, and 3D imaging in biological systems.[18,101,115-118]

3 | CPL BASED ON THERMOTROPIC LCs

The formation of mesophases depends on the temperature variations, where the LC phases appear only in a certain temperature range. These LCs are the thermotropic LCs with rod-like (calamitic), bowl-like, discotic, or bent-core molecular geometry. Generally, the CPL can be introduced into thermotropic LCs using three methods: (1) through fabricating the chiral moiety; (2) by developing a host-guest strategy between the achiral host molecules and the chiral guests. Here, the nematic LCs, mostly made of rod-like molecules, produce cholesteric structures via their doping with chiral elements. Thus, CPL signals can be generated by integrating stimuli-responsive chiral molecules into cholesteric LCs with self-organized helical superstructures, which can selectively reflect light with the same handedness as their helix, resulting in enhanced chirality and high g_{lum} values compared to those of organic micro-/nanostructure systems[84]; (3) CPL is speculated to be generated from the achiral molecules by spontaneous symmetry-breaking, such as achiral C3-symmetry gelators.[93] In addition, the helical nanofilament phases (HNFs), referred to as the B4 phase,[119,120] comprising the bent-core mesogens reveal sorts of smectic phases with twisted layers that maintain the helical structures. The CPL of this phase offers new functionalities with unprecedented behaviors in thermotropic LCs, which is highly promising materials in the field of information and display technology.

3.1 | CPL based on cholesteric LCs

Cholesteric LCs manifest a nonsuperimposable helicoidal superstructure, which were first discovered by Reinitzer in 1888 using the cholesterol derivatives.[121] A cholesteric mesophase comprises thin nematic layers, which are stacked with their directors rotated. The molecules in cholesteric LCs demonstrate the spatial helicoidal orientation along their helical axis, typically characterized by the twist handedness and the helical pitch (p).[39] Handedness is defined by that the orientations of molecular mesogens rotate, either clockwise or anticlockwise, along the helical axis. The parameter p in cholesteric LCs is defined by the distance where the director rotates along the helical axis for a full 360°.[71,122,123] The wavelength of the reflected light at the normal incidence is defined by the equation of $\lambda = np$, where λ is the wavelength of light and n is the refractive index.[124-126] In general, a cholesteric LC exhibits the feature of the Bragg reflection.[127,128] Thus, the reflection band is centered at $\lambda_c = n_{av}p\cos(\theta)$ and the bandwidth can be estimated by the equation of $\Delta\lambda = (n_e - n_o)p$, where Δn is the birefringence of the LC host and θ is the incident angle. n_o, n_e, and n_{av} are the ordinary, extraordinary, and average refractive indices of the LC, respectively.[129] Interestingly, the Bragg reflection in cholesteric LCs is CP, where the helical sense is the same as the helix of cholesteric LCs when the periodicity of the helical structure is compared to the wavelengths of the visible light.[44,130,131] When the incident light interacts with the helicoidal superstructures in cholesteric LCs, CP light with the same handedness as the helix of helicoidal superstructures will be reflected, whereas the opposite handedness can be transmitted from the structures. In addition, the PBG effect[132-134] induced by the helical superstructures of cholesteric LCs is applied in mirrorless band-edge laser resonators.[135] The recent endeavors in the

advancements of cholesteric LCs on CPL have been achieved by mixing a nematic LC with a chiral agent or with the predesigned light-driven MMs, which can be extensively used in several applications, such as chiral sensing, tunable color filters, polarizers, and mirrorless lasing.[136-140] Li et al. used the cholesteric LCs to tune the reversible reflection color ranging from visible to infrared region of the spectrum by fabricating the chiral dopants of the new fluorescent molecular switches.[141]

CPL induced by inorganic dopants

The chiral nanostructures and luminescence characteristics of the CPL-active inorganic nanomaterials, including lanthanide complexes,[142-144] QDs,[101,145] nanoparticles or nanorods,[146] and perovskites,[147] have promoted the fundamental research and encouraged scientists to explore the chiroptical activity of these CPL-active materials. The lanthanide complexes, such as gadolinium (III), terbium (III), and europium (III), demonstrate a high g_{lum}; nevertheless, the photoluminescence quantum efficiency of these complexes is considerably low (<40%).[142-144] QDs, including III−V and II−VI semiconducting and metallic QDs, afford a promising path by attaching chiral ligands to their surfaces to realize CPL using the nanostructure-based technologies. However, the high g_{lum} and photoluminescence quantum efficiency remain a challenge.[148-150] The emerging photovoltaic material of organic-inorganic hybrid perovskites is a breakthrough in the advancement of new chiral semiconductors.[151] Metal-halide perovskite semiconductors fulfill the majority of the requirements of the CPL-emitting sources, which are peculiarly used for LEDs, optical lasers, photodetectors, and high efficiency photovoltaic cells owing to their fascinating optical and electric properties, such as adjustable PBG, remarkable light absorption, and available synthesis of high-quality crystals.[152,153] The CP light is broadly employed in advanced technologies involving 3D displays and information carriers in quantum computation. Therefore, high polarization, well-controlled handedness, and high luminescent efficiency are required for CP light. Luminescence based on halide perovskite nanocrystals is considered in applications of LEDs and solar cells.[154]

Li et al.[87] used perovskite nanocrystals doped in a predetermined handedness cholesteric superstructure to obtain CPL. The perovskite nanoparticle layer was arranged between two filters, whose handedness of the helical structure was opposite. The cholesteric film converted unpolarized light originating from perovskites into CPL with $|g_{lum}|$ up to 1.6. The system configuration for CP emission is made of a light source and two cholesteric filters. The emission layer consisted of perovskite material and cholesteric filters made of left- and right-handed polymeric cholesteric films. Figure 3a reveals the basic principle in the CPL system. The perovskite film produces unpolarized light from both sides in the absence of a cholesteric film (50% up and down). The perovskite film is placed on the right-handed cholesteric LC (R-CLC) film, of which the reflection band coincides with the emission wavelength from perovskites. Once exposed to the ultraviolet (UV) radiation, the polarization of upward light emission remains unchanged, whereas the downward light was reflected with a 180° phase shifting and change in the handedness. Hence, the reflected upward light is RCP, whereas the remaining half turns to be LCP after propagating through the R-CLC film. Similarly, the upward light emission is divided into two equal parts, when an L-CLC film is stacked on the other perovskite films (Figure 3a). Meanwhile, the emission colors of blue (B), green (G), and red (R) are regulated by different amounts of halide compositions and various geometrical sizes. The B, G, and R emission correspond to $CsPbBr_3$, bromide-based perovskite $CsPbBr_3$, and iodine-based perovskite $CsPbI_3$, respectively. Figure 3b shows polarized optical microscope (POM) images of *R*-cholesteric and *L*-cholesteric LC films with different amounts of chiral dopants, signifying that the cholesteric LC film displays planar structures with B, G, and R emission because of Bragg reflection. Figure 3c–e illustrates images of perovskite films with *R*-cholesteric or the *L*-cholesteric LC films under the observation (Figure 3c), a RCP (Figure 3d), and a left-handed circular polarizer (Figure 3e). All perovskite-based cholesteric LCs exhibit bright photoluminescence in the absence of a circular polarizer. When a right-handedness circular polarizer is kept on the top of the glass and an *R*-cholesteric LC film, the LCP light with the opposite handedness can be transmitted through the glass. The polarized filter allows the light with the same handedness to propagate through but prohibits the spread of CP light with a reversed handedness (Figure 3d, left sample). In contrast, the RCP light is allowed to pass through using an *L*-cholesteric LC film (Figure 3d, right samples). When a circular polarizer with left handedness is used, the effect of the color saturation is similar to that in a RCP (Figure 3e). Therefore, the polarization of the luminescence is well-controlled using the cholesteric LC film. The full-color chiral light emission obtained by this proposed method offers new possibilities in photonic devices and optoelectronic field. However, the $|g_{lum}|$ values reported for CP light emission based on perovskite materials are less than the theoretical value of 2, which is due to the instability of perovskite nanocrystals. Therefore, a higher $|g_{lum}|$ can be achieved by stabilizing perovskite nanocrystals in cholesteric LCs compared to those systems of cholesteric superstructure stacks doped with inorganic perovskite nanocrystals directly. Zhu et al.[155] successfully developed a novel CPL system with a $|g_{lum}|$ up to 1.9 using perovskites with a bilayer architecture in chiral LC-based devices for enhancing the stimuli-responsive modulation of CPL (Figure 3f). Incorporating a PAN distinctly enhances the luminescent efficiency, improves the stability of perovskite, and tunes the PBG of chiral LC to cover the perovskite's emission band, resulting in

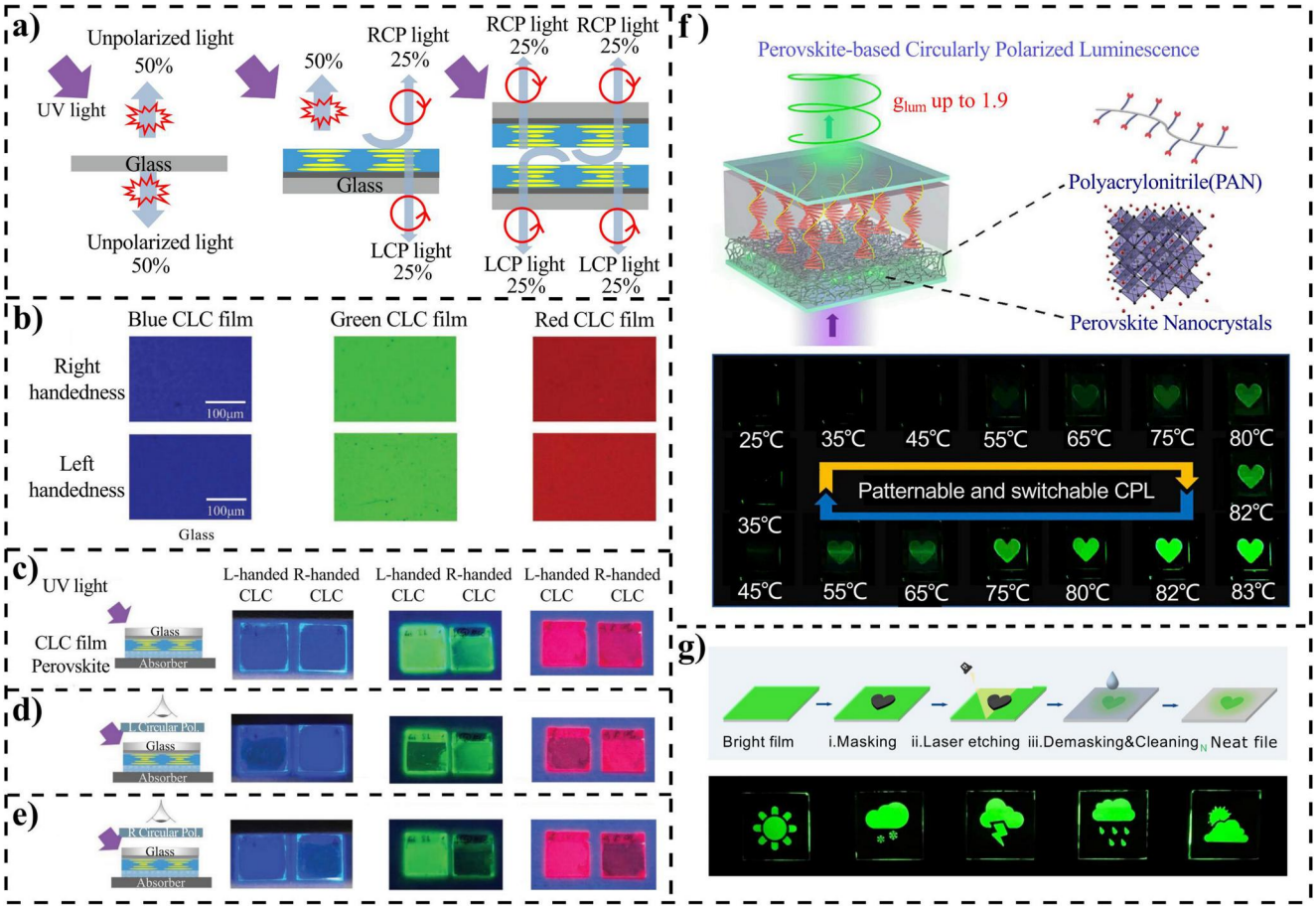

FIGURE 3 (a) Principle of a CPL system. (b) Right- and left-handedness of cholesteric LCs under a POM in the reflection mode. (c–e) Images of perovskite films with R-cholesteric LC or the L-cholesteric LC films observed with the naked eye, an RC polarizer, and an LC polarizer. (a–e) Reproduced with permission.[87] Copyright 2019, Wiley-VCH. (f) The fabrication process of perovskite ($MAPbBr_3$)-embedded polymer films. (g) Photographs of perovskite-embedded polyacrylonitrile films under UV light irradiation. (f–g) Reproduced with permission.[155] Copyright 2022, Elsevier. CPL, circularly polarized luminescence; LC, left-handed circularly; LCs, liquid crystals; POM, polarized optical microscope; RC, right-handed circularly; UV, ultraviolet.

the stable and nearly pure CPL. The rather high $|g_{lum}|$ is due to the matching between the PBG of the chiral LC and the emission peak of perovskite. Thus, chiral luminescent materials and optical modulations are essential for fabricating new CPL-active materials, enabling both the enhanced luminescence efficiency and large $|g_{lum}|$. The perovskite-polymer solution is spin-coating on a flat substrate, followed by a predefined mask etched by the laser. The assembled device can work as a progressive anti-counterfeiting label. When it is irradiated by UV light, the graphical information appears promptly; however, it disappears when covered by a circular polarizer, thereby preventing the transmission of CPL of the same handedness. Several fine graphic patterns, such as sun, snow, thunder, rain, and clouds, are extended under the fabrication route (Figure 3g) to improve the graphical display.

Photon upconversion, which can absorb low-energy photons, but emit high-energy photons, is regarded as an excellent nonlinear-optical phenomenon.[156] The processes of triplet-triplet annihilation (TTA)-related upconversion[157,158] and UNPs[159-165] are the two primary approaches toward upconverted CPL. Duan et al.[113] reported the upconverted CPL relying on the TTA process in 2017. The obtained g_{lum} value under UV irradiation at 360 nm was low (2×10^{-4}), whereas the value of g_{lum} at approximately 450 nm increased to 4×10^{-3}, which was one order of magnitude higher than that at 532 nm. TTA-based upconversion processes and upconverted CPL in the LC system resulted in the enhancement of the g_{lum} by three orders and one order, respectively.[166] The perovskite nanocrystals simultaneously exhibited outstanding absorption and luminescent properties owing to the unique characteristics, such as precisely tunable bandgaps, long charge-carrier diffusion lengths, and high defect tolerance.[167] Particularly, the metal-halide perovskites are the potential light sources for next-generation LED and lasers.[168] Lanthanide-doped UNPs were reported first in 2000,[162] which can convert photons in low energy to photons in high energy via anti-Stokes, thereby enabling a

broad range of practical applications, including high-resolution biomedical imaging, sensing, drug-delivery systems, data safety, and photovoltaic technologies.[161,164,169-171] Duan et al.[172] designed a chiral emissive system by integrating UNPs and perovskites into the cholesteric LC and successfully demonstrated an enhanced upconverted CPL dependent on the radiative-energy transfer (RET) from UNPs to the $CsPbBr_3$ perovskite nanocrystals. The g_{lum} of the upconverted CPL could be amplified to a significantly high value of 1.1 by adjusting the emission peak of the $CsPbBr_3$ perovskite nanocrystals at the center of the PBG in cholesteric LCs. The $CsPbBr_3$ perovskite nanocrystals are utilized as the energy acceptor and UNPs are served as the energy donor, whose emission peak is located at the center and the edge of PBG of cholesteric LC, respectively (Figure 4a). The RET process is turned off under the electric field (Figure 4b,e). The planar texture of cholesteric LC is observed using POM (Figure 4c). The reflection of the cholesteric LC is unable to be detected when the voltage is continuously increased to 100 V, suggesting that the LC molecules prefer to orient parallelly to the direction of the electric field (Figure 4f). The green color (Figure 4c, inset) changes to bluish-violet under laser excitation at 980 nm (Figure 4f, inset) and the emission of the UNPs is quenched by 74% at 100 V (Figure 4d,g). This phenomenon can be explained by that the emission of the UNPs would be suppressed when the chiral superstructure of cholesteric LC is completely destroyed by the strong electric field, which uniformly reorients the LC molecules.

CPL induced by organic dopants

Several studies have been reported on CPL-active materials based on organic molecules, including the axially chiral binaphthyls derivatives, helicenes, and chiral cyclophanes, because of the associated advantages of high fluorescence efficiency, tunable emission wavelength, and precise structure-performance relationship.[84,110,173-177] In addition, organic molecules offer a relatively high g_{lum} by self-organizing into helical polymers or using aggregation-induced emission dyes (AIEs). However, the g_{lum} values obtained at the wavelength of light in the visible region for most of reported CPL-active systems are very low, which restrict the practical applications. Recently, the organic molecules-based LCs in photon upconversion systems have become the frontier of scientific fields.[84,178] Particularly, doping of chiral emitters into the achiral nematic LCs is a preferred method to obtain CPL-active cholesteric LCs. Duan et al.[88] demonstrated a complicated system with intense circularly polarized ultraviolet luminescence (CPUL) of high $|g_{lum}|$ value (0.19), which allowed an enantioselective polymerization, stimulated by chiral UV light. The system was constructed by integrating the sensitized TTA-based upconversion and CPL to explore the upconverted CPUL and the emission from the visible region to the UV region (Figure 5a). In addition, the enantioselective photopolymerization of diacetylene was initiated by the upconverted CPUL (Figure 5b). *R*-TP/4CzIPN and *R*-TP/5CB were used under a light source of the continuous wave laser to generate an upconverted CPUL emission. The complex *R*-TP/4CzIPN/5CB was illuminated using 445 nm CW laser; subsequently, the thin 2, 4-nonadecanediynoic acid (NA) films were located behind the sample with a filter located in the middle. After exposing to the upconverted CPUL for a small duration, the NA film became blue, signifying the formation of polydiacetylene. The CD signal of polydiacetylene films after exposing to the upconverted CPUL was produced by *R*-TP/4CzIPN and *S*-TP/4CzIPN in cholesteric LC, which demonstrates a mirror-image Cotton effect (Figure 5c). The photopolymerization of NA was repeated in 10 different batches to ensure the reliability of the enantioselectivity. The black and red spheres in Figure 5d represent the absorption dissymmetry factor g_{CD} of polydiacetylene generated from *R*-TP/4CzIPN/5CB and *S*-TP/4CzIPN/5CB, respectively. The CD signals with mirror images at 640 nm indicate that the chirality of polydiacetylene follows the molecular chirality of the annihilator (Figure 5d). This result signifies that polydiacetylene was fabricated via the enantioselective polymerization.

The self-assembly of LCs is promising for constructing stimuli-responsive materials by utilizing heat, light, or chemicals stimuli, thus offering underlying applications in deployable soft actuating devices.[179,180] Li et al.[138] reported the 3D control of the helical axis of a cholesteric LC coupled with the reversal of its handedness merely by light. Furthermore, Li et al.[41,181] discussed a series of developments on the reversal of the handedness in cholesteric LCs by different photoisomerizable chiral molecular switches. Yang et al.[182] constructed a chiral-switchable device comprising a dynamic superstructure of cholesteric LCs doped with a light-driven MM to achieve the concurrent chirality and intensity modulations of CPL (Figure 6a). The MM was specially designed with an alkyl chain substituent to improve the dopant-host compatibility, thereby allowing for advanced chemical isomerization under UV light. The rotary of these motors can alter the handedness by altering the self-assembled structures of cholesteric LCs. Four guest achiral luminescent dyes (BHA, DAC, N-R, and R-6G) were selected (Figure 6b) to be doped in cholesteric LCs. The reflection wavelength of cholesteric LCs was shifted using UV-light. CPL signals could be regulated by locating the emission wavelength at the edges of the PBG, such as doping the various concentrations of R5011 and enlarging the amount of MM. Subsequently, the only photoswitchable MM was doped in SLC1717 to obtain the reversible chiral inversion cholesteric superstructure. The handedness is supposed to be validly changed from left-handed to right-handed upon irradiating with UV at 365 nm (Figure 6d) and subsequently recovered to the initial condition when the superstructure was heated or kept at 25°C. The maximum g_{lum} value of 0.42 was obtained and

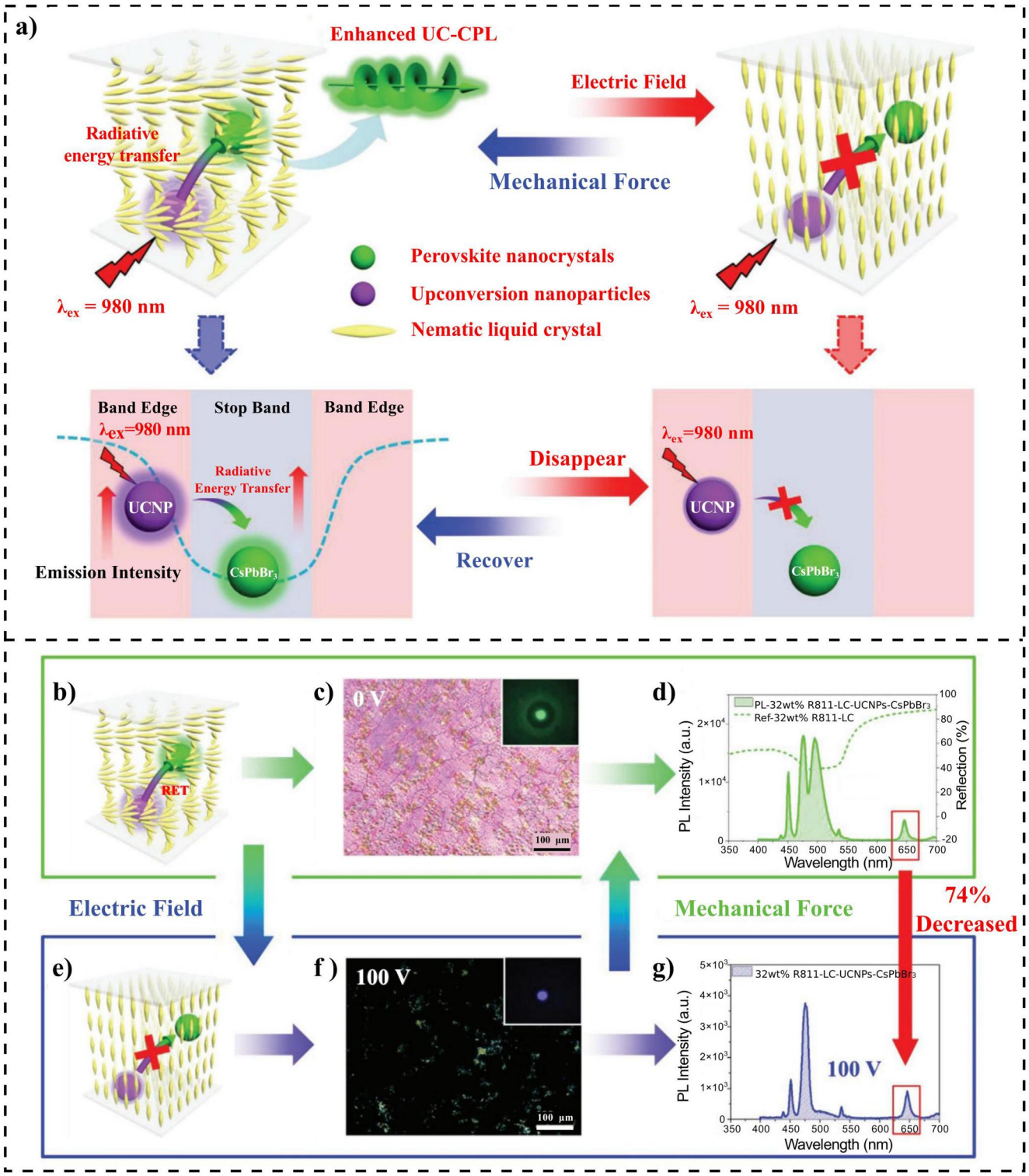

FIGURE 4 (a) Upconverted CPL through the RET process. (b) Schematic of the RET process from UNPs to $CsPbBr_3$ perovskite nanocrystals in the cholesteric LC at 0 V. (c) Planar texture of the cholesteric LC using the POM. (d) Upconverted emission in both the $CsPbBr_3$ perovskite nanocrystals and UNPs. (e) Schematic of the process of RET transfer from UNPs to the $CsPbBr_3$ perovskite nanocrystals when it is switched off upon the voltage of 100 V. (f) No reflection of cholesteric LC in POM. (g) Detection of only weak emission of the UNPs. Reproduced with permission.[172] Copyright 2020, Wiley-VCH. CPL, circularly polarized luminescence; LC, liquid crystal; POM, polarized optical microscope; RET, radiative-energy transfer; UNPs, upconversion nanoparticles.

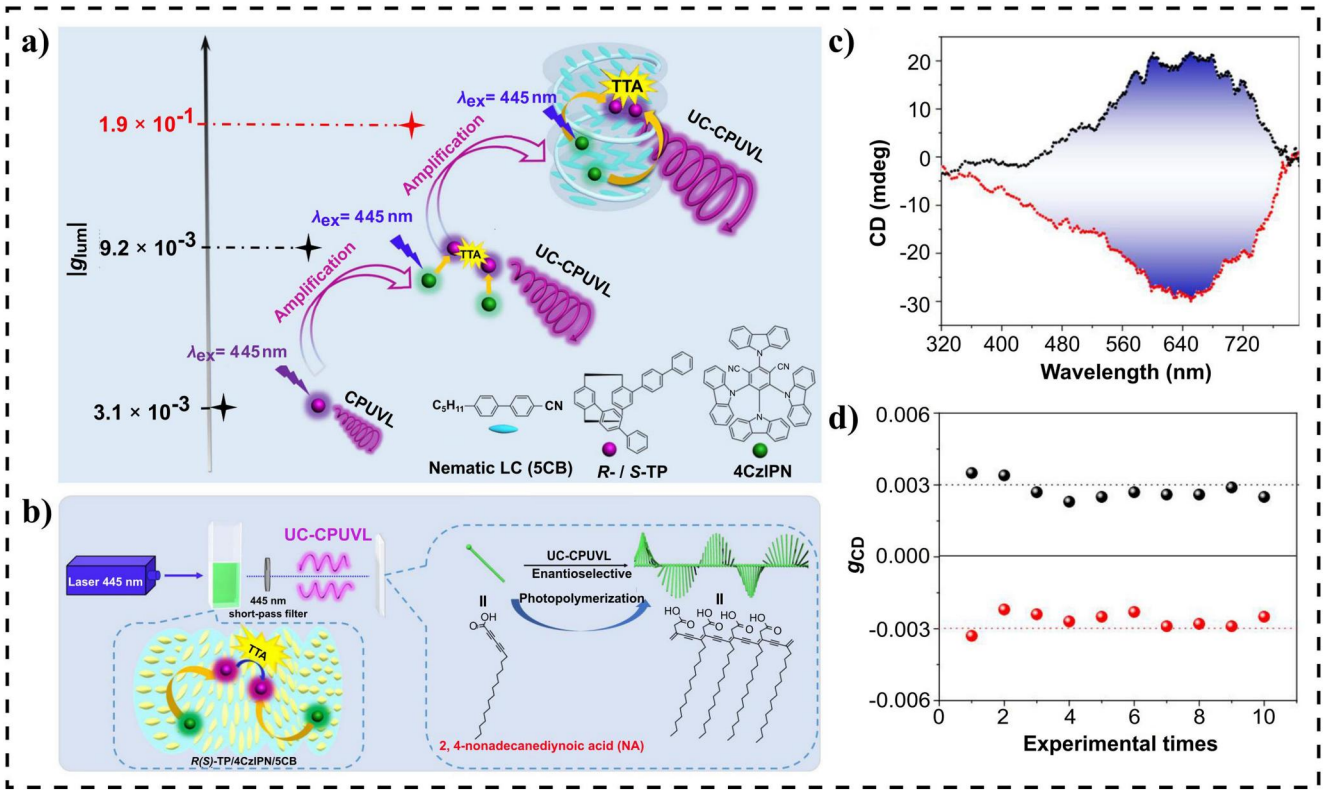

FIGURE 5 (a) Process of consecutively amplified CPUVL. (b) Schematic of the enantioselective photopolymerization of NA. (c) CD of polydiacetylene films after exposing to the upconverted CPUVL. (d) Absorption dissymmetry factor g_{CD} of the chiral PDA in 10 different batches. Reproduced with permission.[88] Copyright 2020, Springer Nature. CD, circular dichroism; CPUVL, circularly polarized ultraviolet luminescence; NA, 2, 4-nonadecanediynoic acid; PDA, polydiacetylene.

the reversed handedness of CPL was repeated back and forth for many times without any associated concerns (Figure 6e). The stimuli-responsive principle of reversible CPL was designed using the cholesteric LC, which adds a significant value in new possible applications for optoelectronic and photonics.

3.2 | CPL based on bent-core LCs

Chiral LC phases formed by bent-core molecules have achieved widespread concerns owing to their distinct polarity.[183] The chirality and spontaneous polar order break the symmetry, coupling to drive the layer to undergo the saddle-splay deformation,[184] forming a spectacular hierarchical structure of the twisted layers.[119] Since the chiral resolution and the polar switching were discovered in bent-core LCs, several studies have investigated new LCs comprising bent-core molecules and their unique phase behaviors, orientational control of HNF growth,[185-190] and excellent gelation ability.[191] At least eight different smectic phases made of bent-core molecules have been found, which are named as B1–B8 phases,[192] where "B" stands for "bow-shaped," "bent-core," "bent-shaped," or "banana-shaped."[193] The B4 phase or HNFs[55,185-189,194] of bent-core compounds was first resolved with freeze-fracture transmission electron microscopy by Clark in 2009.[119] Figure 7a illustrates the mechanism of the formation of HNFs. The spectacular hierarchical structures of HNFs originate from achiral bent-core molecules. The projection of two arms of bent-core molecules in the midplane did not match; the tilt directions projected on the layer midplane are almost vertical, which result in the saddle-splay layer curvature and form nanofilaments of the twist smectic layer. Walba[120] reported that the modulated HNFs (HNF_{mod}s) had in-layer modulation apart from the negative curvature of layers. The textures in the B4 phase are transparent blue color[197] (in the reflection mode) under crossed polarizers observed by naked eyes, reason of which is not completely understood, though it is certainly related to scattering, reflection, and interference by packing of these filaments in thin films.[198] For example, Jákli et al.[199] reported that the filaments in HNFs with a second twist were not parallel to each other; instead, they were rotated with respect to each other by an angle of 35–40°, which explains the color of HNFs. Clark et al.[200] reported the nanophase segregations in binary mixtures of a bent-core LC and a rod-like LC at a low temperature. Based on these studies, Choi et al.[195] demonstrated a similar approach to achieve CPL by self-assembled chiral supernanospace of achiral bent-core molecules. The achiral mixture in which a bent-core LC as the host and rod-like LC with a fluorescent dye as the guest

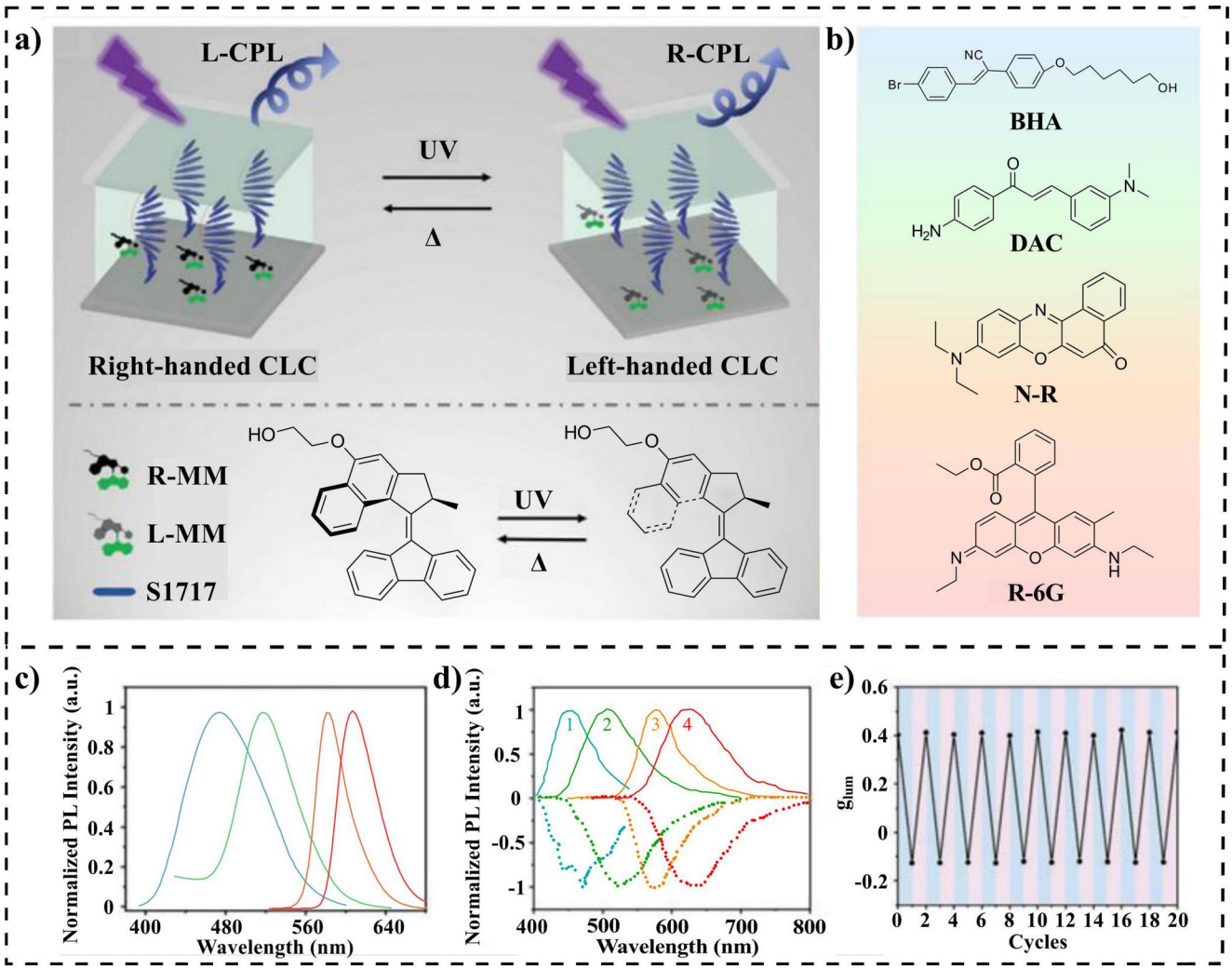

FIGURE 6 (a) Schematic of photo-driven chiral inversion of CPL in cholesteric LCs. (b) Structures of 4 types of luminescence dyes. (c) Fluorescence spectra of dyes in THF. (d) Mirror images of CPL of various cholesteric LCs. (e) Changes of the g_{lum} during the process of several photoisomerization and thermal recovery cycles of the BHA film. Reproduced with permission.[182] Copyright 2022, Wiley-VCH. CPL, circularly polarized luminescence; LCs, liquid crystals; THF, tetrahydrofuran.

(host: P12, guest: 5PCB) was investigated. The nematic phase blended with the fluorescent dye was segregated from HNFs, thus creating the chiral nanospace. Therefore, CPL signals were detected from the dye blended with rod-like molecules. Apparently, CPL signals are not observed in the nematic LC formed by rod-like molecules with the absence of chiral nanospace (Figure 7b). The approach for CPL generation can be fulfilled by using molecular chirality or complicated molecular design comprising chiral dopants, chiral fluorophores, chiral templates, and chiral gelators. In addition, the superstructure of the bent-core LCs allows to modulate the g_{lum} ($\sim 10^{-3}$) by external stimuli, such as electric field, which can be used to control the reorientation or nonlinear nonequilibrium state of the nematic molecules.[201,202] These observations provide a direct evidence of the spontaneous chiral aggregation of rod-like molecules, which are segregated from HNF networks and motivate us to construct highly dissymmetric CPL and practical CPL-active materials. Furthermore, Choi et al.[52] designed the inversed HNF networks, which were used as a chiral nanotemplate to confine nematic LCs. A helical nanofilament was utilized as three-dimensional mold to create an inverse nanohelical structure. Subsequently, the achiral nematic LCs doped with fluorescent dye were refilled in the chiral nanoporous film, accompanied by the chirality transfer from the inversed HNFs to nematic LCs, which exhibited stimuli-responsive CPL with a low g_{lum} value in the order of magnitudes of 10^{-3}.

Several approaches have been investigated to acquire highly efficient CPL-active materials for increasing $|g_{lum}|$ in the helical nanofilaments. Shadpour et al.[196] designed a CPL-active material using HNF_{mod}s with axially chiral binaphthyl-based additives, which were confined in anodic aluminum oxide (AAO) nanochannels (Figure 7c). Interestingly, the handedness of the bulk HNF_{mod}s is not affected by the chiral additives, which are expelled from HNF_{mod}s,

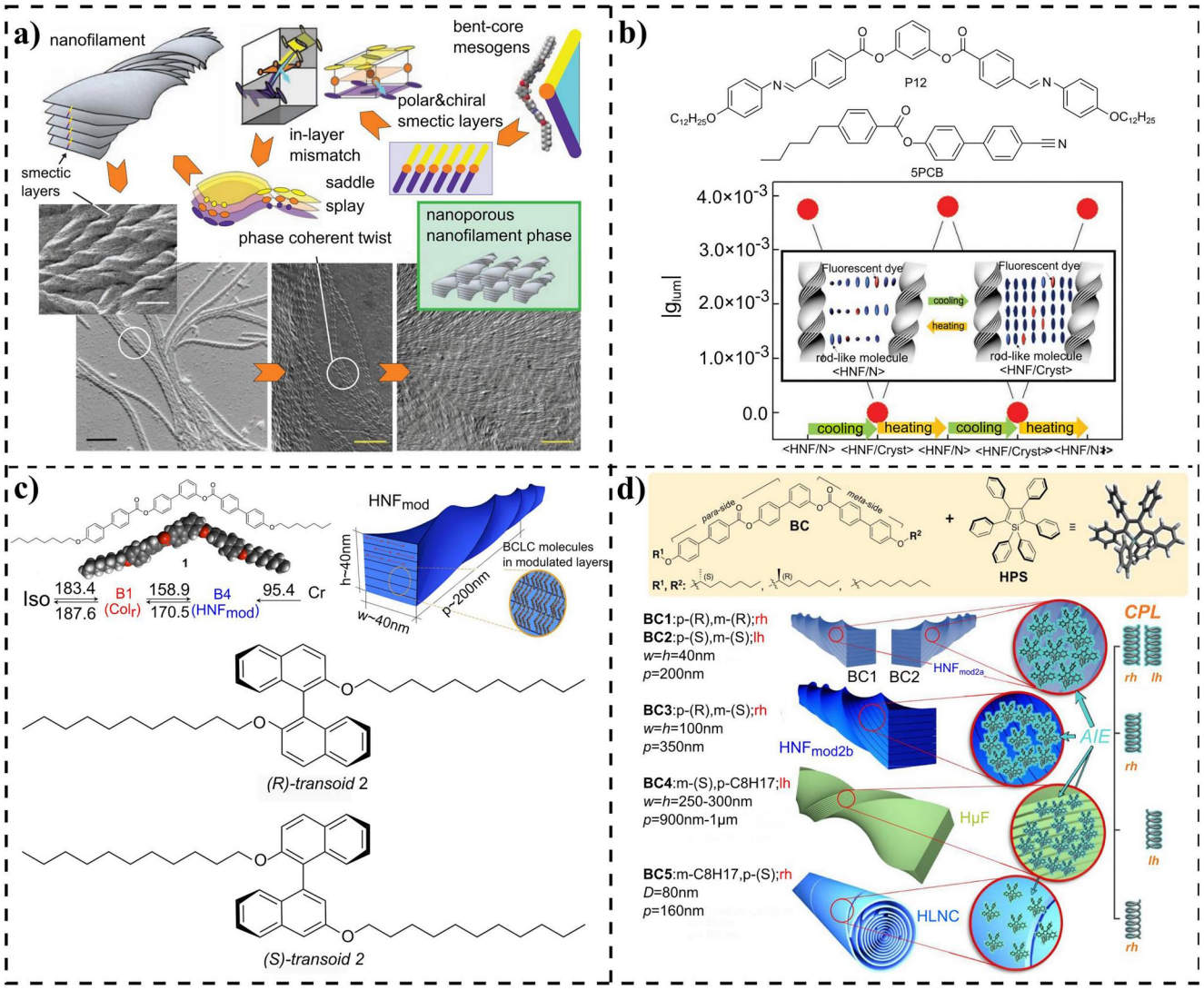

FIGURE 7 (a) Hierarchical self-assembly of the nanofilament phase. Reproduced with permission.[119] Copyright 2009, American Association for the Advancement of Science. (b) Reversible modulation of $|g_{lum}|$. Reproduced with permission.[195] Copyright 2019, Wiley-VCH. (c) Chemical structure, phase sequence of the BCLC host 1, and chemical structures of chiral binaphthyl guests. Reproduced with permission.[196] Copyright 2020, American Chemical Society. (d) Bent-core LCs BC1–BC5, forming a range of B4 morphologies, doped by HPS. Reproduced with permission.[89] Copyright 2022, American Chemical Society. BCLC, bent-core liquid crystal; HPS, hexaphenylsilole; LCs, liquid crystals.

consequently resulting in the chirality preserving growth. However, the value of g_{lum} remains low in this supramolecular structure based on HNF$_{mod}$s because of the existence of the domains with opposite handedness and the arbitrary arrangements of HNF$_{mod}$s. Similarly, Cheng et al.[203] doped chiral binaphthyl-based inducers into achiral LCs polymers to fabricate chiral co-assemblies and investigate CPL behaviors by regulating helical nanofibers in the supramolecular co-assembly process. Thus, the chirality could be efficiently transferred from the helically assembled supramolecular system.[204] Recently, Liu et al.[89] constructed a thermal-driven tunable CPL-active system using helical nano-[205] or microfilament[206] templates in conjunction with hexaphenylsilole (HPS), which relied on a supramolecular self-assembly approach (Figure 7d). Tang et al.[207] first reported luminescent compounds with AIE property in 2001. Since then, significant research studies have been probed into CPL-active materials, which are based on AIEgens ranging from small molecules, polymers, and self-assemblies to hybrids.[93,147,208-212] AIEgens could modify and regulate the self-assembly in agglomerates to obtain the excellent optical properties[213] and provide desirable properties because of their strong emissivity in the aggregated state, whereas they remain nonemissive in organic solvents.[214-219] Furthermore, bent-core LCs were demonstrated, which could form helical (heliconical) nano- or microfilaments of B4 phase[205,206] by doping AIE and confinement in the appropriate diameter of AAO,[220] to ensure the arrangement of HNFs in the same direction. Particularly, the same handedness of these nano- or

microfilament templates was chosen by adding the chiral centers in the flexible chains to avoid the destructive effect of the racemization. Additionally, the mechanism of HPS[215] was proposed based on nonplanar luminogenic molecules by restricting the free intramolecular rotation of phenyls in the aggregate state, which served as a chiral additive to induce a small pitch as the binaphthyl derivatives. Thus, the pitch was reduced by 35% compared with that in the case of not doping chiral additives or efficient HPS aggregations in AAO. The intrinsic geometric differences (height, width, and helical pitch) of the B4 templates and differences in exposed aromatic areas led to different CPL activities. Thus, an efficient method is to design chiroptical materials with high $|g_{lum}|$ (reaching up to 0.25) by optimizing three factors, including chiral centers, HPS, and AAO in the system. This approach will provide new ideas into the construction of temperature-rate indicators by combination of AIE dyes. The similar approach was employed in AIE-active dyes to obtain CPL by the supramolecular self-assembly process in the cholesteric LC or smectic C* system.[221] The chiral binaphthyl enantiomers and AIE dyes[218,222] or AIE-active binaphthyl derivatives[223] were compatibly doped into a nematic LC to produce the new AIE-cholesteric LCs, which can induce strong CPL responses with high $|g_{lum}|$. Tang et al.[224,225] constructed CPL-active AIEgens by locating AIEgen into chiral cholesterols to form chiral LCs, which enable the increase of the emission efficiency and also provide a useful platform to obtain high g_{lum}.

The arrangement of metal nanoparticles in the LC-nanoparticle hybrid systems provides potential opportunities to broaden the variety of LC's characteristic responding to the external stimuli due to new optical activity of plasmon coupling. Marcverelst et al.[226] demonstrated the long-range ordering of nanoparticle assemblies, which successfully follow the helical configuration of cholesteric LC. A significant amount of reported studies on LCs as templates is related to nematic, smectic, and BPs.[227-230] Cholesteric LCs have been widely explored including chirality amplification by functionalized nanoparticles to nanorods[29] and the effect of nanoshape and solute-solvent compatibility toward chirality transfer in nematic LCs.[28] Li et al.[231] functionalized SiO_2 nanoparticles with a mesogenic monolayer on the surface to promote the compatibility in an LC and probed into their influence on electro-optical properties of a dual-frequency system. Recently, HNFs have been selected as chiral LC templates for designing CPL nanomaterials due to their switching ability of temperature-driven structural changes. Meanwhile, nanoparticle-based materials are designed through self-assembly of the anisotropic nanoparticles into 2D or 3D assembly to obtain the unique optical properties of the devices at the macroscale.[50] Lesiak et al.[53] presented an approach by doping gold nanoparticles into a spatial confinement of a nematic LC to self-induce a one-dimensional photonic periodic structure. The periodicity of this structure can be dynamically adjusted, accompanied by the tunable wavelength, adjustable spectra width, and a narrow transmission band. This process was not only reversible but also could be regulated by changing the diameters of the confining space, thereby probably allowing the fabrication of the adjustable and broad range of photonic devices, such as tunable filters or reflectors, and light shutters. Intriguingly, Jung et al.[232] generated the helical nanoparticle superstructures by assembling the helical nanofiber templates. The size of gold nanoparticles within the helically organized superstructures can be regulated, and the nanoparticle organizations enable the predictable chiroptical properties based on the expected surface plasmon absorption wavelength of the chiroptical materials. Lewandowski et al.[51,233] used HNFs to regulate the plasmonic nanoparticles with accurately tunable nanostructures. The interaction of plasmonic nanoparticles and HNFs resulted in the formation of hierarchical helical nanostructures (Figure 8a,b). The nanoparticles were particularly functionalized with chemically compatible organic ligands to maintain the sufficient solubility and chemical compatibility between the nanoparticles and the HNFs. When helical nanostructures started growing as a function of cooling rates, the assembly of functionalized nanoparticles into helical structures could be driven. Subsequently, the nanoparticles were expelled from the bulk to the boundary of the sample because of the location of the nanoparticles at the phase boundaries. The versatility was confirmed by blending the supramolecular nanofibers with small spherical nanoparticles (Figure 8c–f) and nanorods (Figure 8g–j), resulting in an actively tunable structure of helical nanocomposites, as observed by transmission electron microscopy (TEM), which was performed to figure out the Au1-3/L-L helical structure. Hence, the approach of employing HNFs as templates to fabricate chiral plasmonic and CPL-active material by chiral dopants confirmed an effective approach, which can open a new way toward co-assembly systems.

4 | CPL BASED ON LYOTROPIC LCs

QDs[234-239] or carbon dots[240-244] have received significant concerns on account of their outstanding properties and applications in different research fields.[236,238,241,244-246] Many challenging issues associated with doping QDs in cholesteric LCs still exist, such as complex synthesis procedures, elemental shortages, or intrinsic toxicity due to the use of heavy metal, and weak CPL with $|g_{lum}|$ in the range of approximately 10^{-3}–10^{-2}.[20,240,247] For example, Nabiev et al.[248] developed LC-based optical materials by doping fluorescent CdSe/ZnS QDs in cholesteric LCs, in which the CP emission with g_{lum} can be electrically controlled by the helical conformational changes of LC matrices. Balaz et al.[148] designed the CdSe QDs, which can induce CD and CPL by functionalized ligands. MacLachlan et al.[238] encapsulated CdS QDs into the chiral nematic mesoporous silica, which developed an iridescent and luminescent silica-encapsulated CdS QD film. Carbon dots with unique

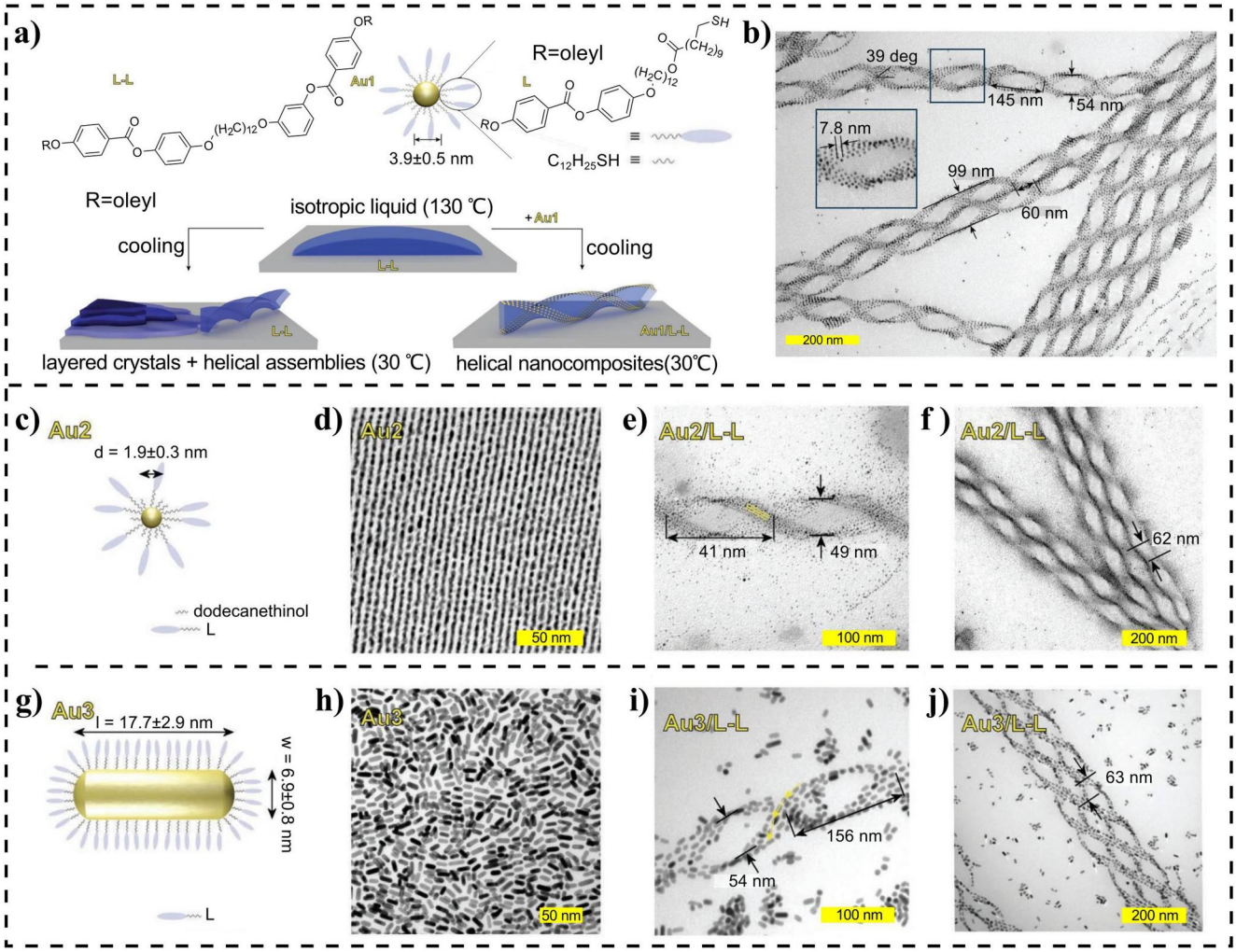

FIGURE 8 (a) Cooperative self-assembly of Au1 nanoparticles and L–L LC. (b) TEM images of Au1/L–L sample. (c) Scheme of Au2 nanoparticles. (d) TEM image of heat annealed Au2. (e, f) TEM image of an Au2/L–L sample. (g) Scheme of Au3 nanoparticles. (h) TEM image of heat-annealed Au3. (i, j) TEM image of an Au3/L–L sample. Reproduced with permission.[51] Copyright 2019, Wiley-VCH. LC, liquid crystal; TEM, transmission electron microscopy.

characteristics, such as photoluminescence, photostability, and biocompatibility,[241,244] are remarkably promising for light-emitting devices, energy storage, optoelectronic applications,[241] bioimaging, and sensing.[246] Lyotropic LCs are the substances that only form LC phases in solvents, where their phase behaviors are closely dependent on the concentration, temperature, pH, and ionic strength. Lyotropic LCs have been observed in many biomolecules, such as DNA,[249,250] lipids,[251] and cellulose,[251] which provide various drugs for diagnosis as well as innovate the market of technologies for medicine and cosmetology.[252] Furthermore, the cellulose nanocrystals (CNCs), the most abundant renewable organic material, can be produced from plants, tunicates, or bacteria.[125,197,253-255] CNCs are chiral with screw-shaped morphology because of the presence of D-glucose.[256] Their surfaces are covered with hydroxyl groups that induce the interparticle attraction in water suspension via hydrogen bonding,[253] resulting in the formation of large clusters in suspensions for individual CNCs.[257] When CNCs are treated with sulfuric acid, they get negatively charged sulfate half-ester surface groups, thereby forming stable colloidal dispersions by self-assembling in water as a consequence of the electrostatic repulsion. Interestingly, for CNCs, when exceeding the critical concentration, they will spontaneously organize into chiral nematic lyotropic LCs[257] by stacked layers of oriented CNC spindles. In addition, when the pitch of CNCs is compared to the wavelength of visible light, the thin films can selectively reflect LCP light and appear iridescent color, which can be applied in optical filters, solar gain regulators,[258-260] and stimuli-responsive stretchable optics.[254] Gao et al.[261] built a luminophore-chiral CNC interface to obtain dual-mode CP light emission; thus, LCP and RCP can emit easily without applying any harsh condition. In addition, CNCs can be used as a chiral nematic template, such as nanoparticles, QDs, carbon dots, and dyes, and can be co-assembled into the functional chiral films.[245,261] Xu et al.[241] fabricated CPL carbon dots (CNC-CDots) of left-handed helical

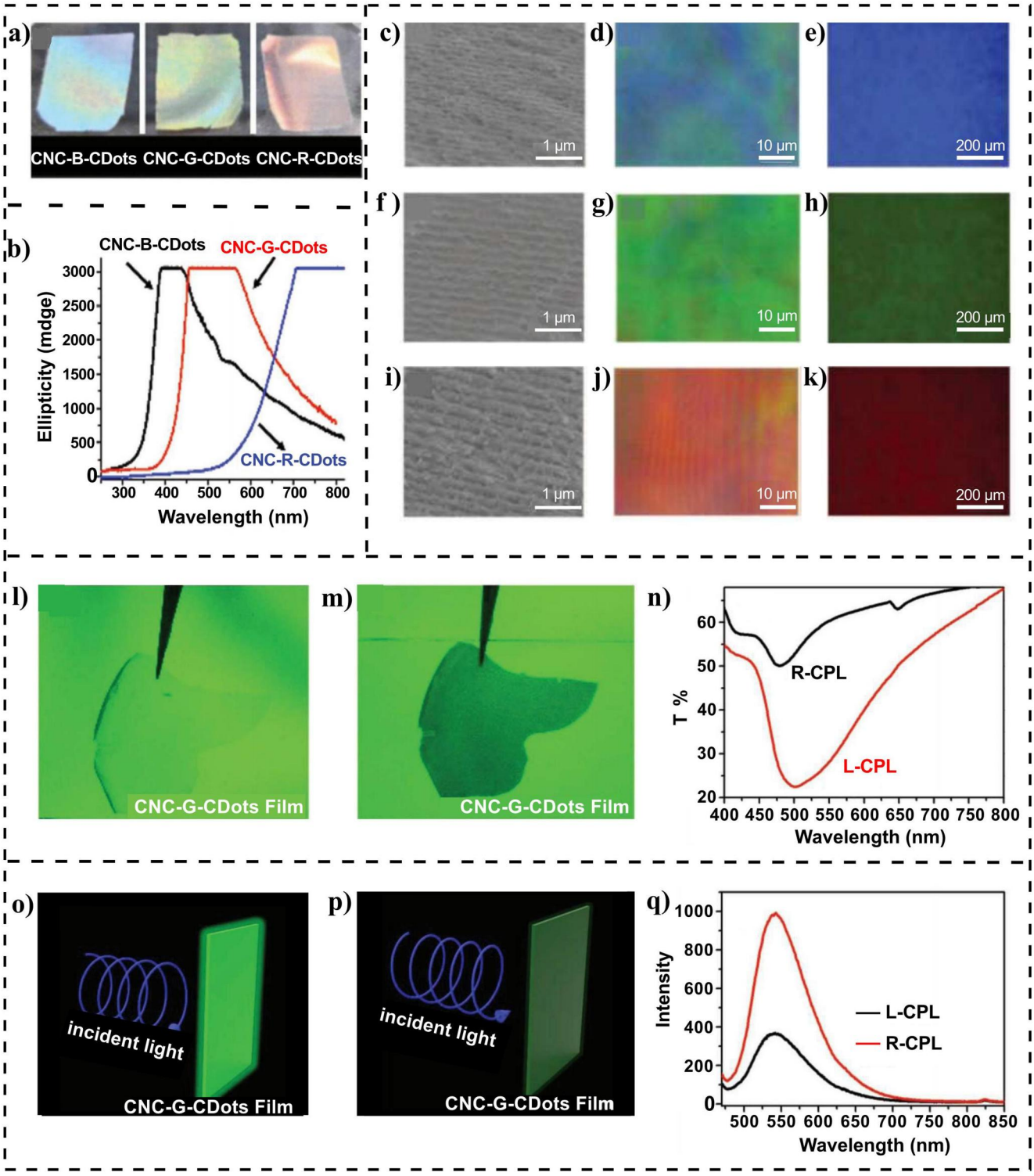

FIGURE 9 (a) Characterization of CNC-B-CDots, CNC-G-CDots, and CNC-R-CDots. (b) CD spectra. (c, f, i) SEM images. (d, g, j) POM images. (e, h, k) Fluorescence microscopy images. CP light using CNC-G-CDots-483 (l, m) upon incident of RCP and LCP light, respectively. (n) Transmission spectra of the film with LCP and RCP light. (o, p) CNC-G-CDots-483 with RCP and LCP light, respectively (q) The corresponding photoemission spectra. Reproduced with permission.[241] Copyright 2018, Wiley-VCH. CD, circular dichroism; CP, circularly polarized; LCP, left-handed circularly polarized light; POM, polarized optical microscope; RCP, right-handed circularly polarized light; SEM, scanning electron microscopy.

superstructures with a tunable PBG from the near-UV to the near-infrared, the multicolor and right-handed CPL with g_{lum} reach up to −0.74. CNC-CDot films were iridescent under natural light. The transmission spectra exhibit three-color reflection band at different wavelengths for CNC-based CDots (Figure 9a). CD spectra demonstrate strong positive

cotton effect, indicating a left-handed CNC-CDot (Figure 9b). The helical pitch of the periodic layer structures is hundreds of nanometers by scanning electron microscopy (Figure 9c,f,i). The fingerprint textures of chiral nematic characteristics and different orientational domains in CNC-CDots are observed using POM (Figure 9d,g,j). The oppositely charged CNCs and CDots attract each other owing to the electrostatic attractions and subsequently lead to the formation of CDots-coated CNC nanorods. In addition, the like-charged CDots repel each other, thereby facilitating a homogeneous distribution and reducing the effect of the fluorescence quenching. The color homogeneity is confirmed by the images from fluorescent microscopy (Figure 9e,h,k). The CNC-G-CDots-483 film appears clear when it is irradiated with 450 nm RCP light. Conversely, the film becomes dark when it is irradiated by 450 nm LCP light (Figure 9l,m). A higher transmittance is observed for the film probed with RCP light than that with LCP light, owing to selectively transmitting 450 nm RCP light by the left-handed CNC-G-CDots-483 (Figure 9n). Noticeably, the CP light can be monitored by performing the photoemission spectra (Figure 9o,p). The transmitted light intensity of the film irradiated by the LCP is largely attenuated owing to the left-handed CNC-G-CDots-483, thus reducing the photoexcitation energy and giving rise to relatively lower emission intensity (Figure 9q). These Cdots open up new fields on the PBG-based CPL and their potential applications in the CP light detection.

Akagi et al.[262] fabricated a CPL-switchable device using a chiral-disubstituted LC-based polyacetylene film with a thermotropic cholesteric LC to dynamically switch and amplify CPL signals. The selective reflection band could be tuned to overlap with the CPL emission band, which facilitates promising applications in optical devices and switchable low-threshold lasers. Akagi et al.[90] synthesized various disubstituted LC polyacetylene derivatives, which can exhibit both lyotropic and thermotropic LC behaviors by doping chiral additives (Figure 10a). The POM analysis depicts the lyotropic LC formed by (***S***)-PA2 with polymer chains spontaneously forming a helically twisted structure, which is prepared using a 10 wt.% solution with toluene (Figure 10b). X-ray diffraction demonstrates a reflection peak at the position of 15.0 Å, indicting the distance of the polymer interchain within a cholesteric LC domain. While POM of (***rac***)-PA2 shows the typical schlieren textures (Figure 10c, left), the previous nematic LC of (***rac***)-PA2 is turned into cholesteric LC after adding the chiral dopant of (***S***)-D1 at 10 wt.% (Figure 10c, right) as evidenced by a fingerprint texture.[263] The (***R***)-PA2 with *P*-helicity exhibits the handedness opposite to the (***S***)-PA2 from the CPL signal with g_{lum} values in the order of 10^{-1} (Figure 10d), thereby prompting a rather high degree of circular polarization in conjugated polymer systems. This is attributed to the chain structures of the disubstituted LC polyacetylene and chirality induced with chiral dopants, leading to a highly ordered lyotropic cholesteric LC. The obtained cholesteric LC promotes the formation of the helically π-stacked disubstituted LC polyacetylene, in which the chirality can be induced by substituting the chiral parts to side chains. Lyotropic cholesteric LCs are regarded as prospective materials possessing the CPL functionality in organic optoelectronic devices.

5 | CPL BASED ON LC POLYMERS

Several endeavors have been made to fabricate CPL-active materials with LC polymers, which exhibit practical applications with a high g_{lum} and luminescent efficiency owing to their excellent thermal stability, processing capacity, and film-forming performance.[66,88,92,203,221,264-273] Generally, two essential approaches are used to endue luminescent polymers with CPL properties, including doping polymers with fluorescence into a cholesteric LC matrix or doping chiral additives into the fluorescent LC polymer matrix,[221,274,275] non-doped chiral π-conjugated polymers,[264,276-280] or helical backbone.[281,282] These advanced technologies pave various novel ways to enhance CPL. One of the promising ways is the addition of LCs to the chiral conjugated polymers.[91,92,264,271] Polymeric cholesteric LCs have received a broad interest in regulating CPL behaviors owing to their good structural integrity, mechanical stability, and processability. Introducing chiral mesogens to form LC polymers is one of the common approaches to fabricate cholesteric LC polymers,[283-287] whereas an achiral smectic LC polymer can often exist owing to the damage of the chiral superstructures during the process. Xiong et al.[91] designed polyether-based cholesteric LC copolymers comprising chiral and nematic LC monomers and cross-linkable agents, which are confined in cholesteric LC elastomers by photo-cross-linking. Subsequently, the strong CPL with high g_{lum} is generated by doping different dyes in cholesteric LC thin films (Figure 11a). Chiral LC polymers have been viewed as one of the most potential CPL materials.[179,285,286,288] Cheng et al.[203] developed a CPL-active material of helical nanofibers using three achiral LC polymers and an axial chiral binaphthyl with anchored dihedral angles to fabricate chiral supramolecular assemblies. The binaphthyl derivatives remarkably favor the rigid planar conformation, which can significantly enhance the amplification of molecular chirality.[259,289-291] The strong CPL emission is achieved through chiral co-assembly, which is attributed to the intermolecular π-π stacking and helical nanofibers formation (Figure 11b). Yang et al.[66] constructed the structurally colored polymer films via the photopolymerization of cholesteric LC mixtures using acrylate mesogens doped with AIE-active dye of tetraphenylethylene and other chiral dopants. The obtained polymer films demonstrate a CPL with high g_{lum} up to 0.58 (Figure 11c).[289-292] These structurally colored polymer films are considerably potential candidates for optical anti-counterfeiting. Generally, nematic LCs are exclusively used as the host in the asymmetric polymerization,[293,294] while smectic LCs with a higher degree of order than nematic LCs can afford the polymers with a higher-order helical structure,

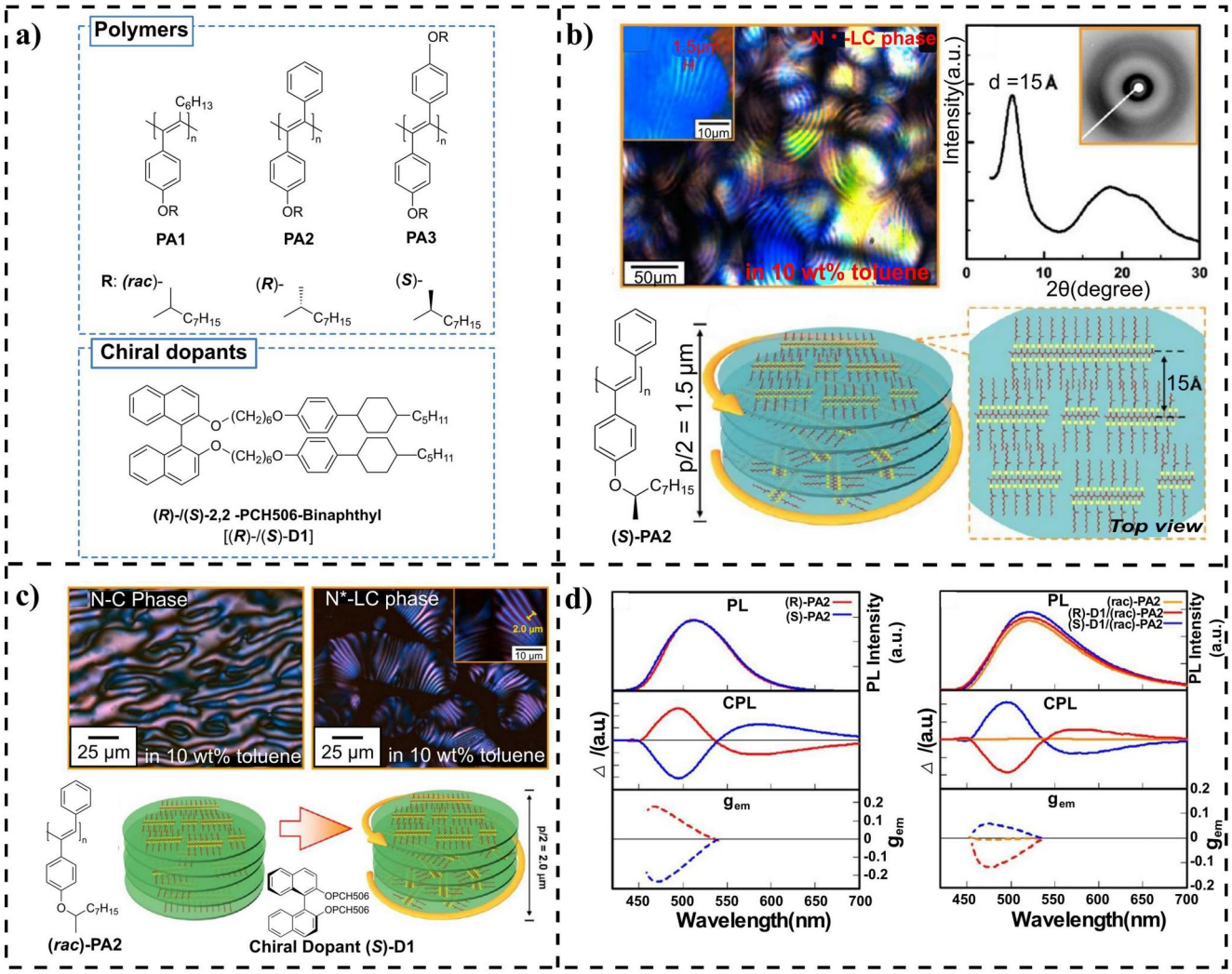

FIGURE 10 (a) Structures of the LC polyacetylene derivatives and chiral dopants. (b, left) POM image of cholesteric LC with (***S***)-PA2 in toluene. (b, right) XRD pattern of (***S***)-PA2. (c, left) POM image of the nematic LC with (***rac***)-PA2 in toluene. (c, right) POM image of cholesteric LC of chiral dopant (***S***)-D1 and (***rac***)-PA2 in toluene (d) PL, CPL, and CPL dissymmetry factor (g_{lum}) spectra of corresponding cholesteric LC film. Reproduced with permission.[90] Copyright 2019, Wiley-VCH. CPL, circularly polarized luminescence; LC, liquid-crystalline; PL, photoluminescence; POM, polarized optical microscope; XRD, X-ray diffraction.

which has rarely been explored yet. Akaji et al.[92] constructed a system using radical photo-cross-linking polymerization in chiral smectic C to obtain the helical network polymers, which produces CPL with high g_{lum} (Figure 11d). Those LC polymers certainly unfold a novel vision to fabricate CPL-active materials, which provide a new direction for the fabrication of CPL-active materials with high performance and significantly enlarge the scope of their practical applications.

6 | APPLICATIONS

CPL has opened new possibilities for the promising applications in chiral sensing, enantioselective syntheses, nonlinear photonic devices, and organic LEDs.[59,67,95] Liu et al.[67] launched the enantioselective polymerization of diacetylene using lanthanide-doped UNPs in the organic-inorganic co-assembled system. Li et al.[137] designed thermally driven cholesteric LC diffraction gratings by integrating a chiral molecular switch into an achiral LC, which can exhibit reversible in-plane orthogonal switching upon temperature and electric field stimulates. Akagi et al.[288] fabricated a thermal-driven chiral-switchable device for CPL using a light-emitting conjugated polymer film and a double-layered cholesteric LC with opposite handedness. The new cholesteric LC systems reveal that temperature can be used to control the selective reflection and allow thermal chirality-switching. Xu et al.[65] fabricated cellulose films with chiral photonic property that allows the right-handed and left-handed passive CPL and right-handed CPL emission owing to the PBG and the

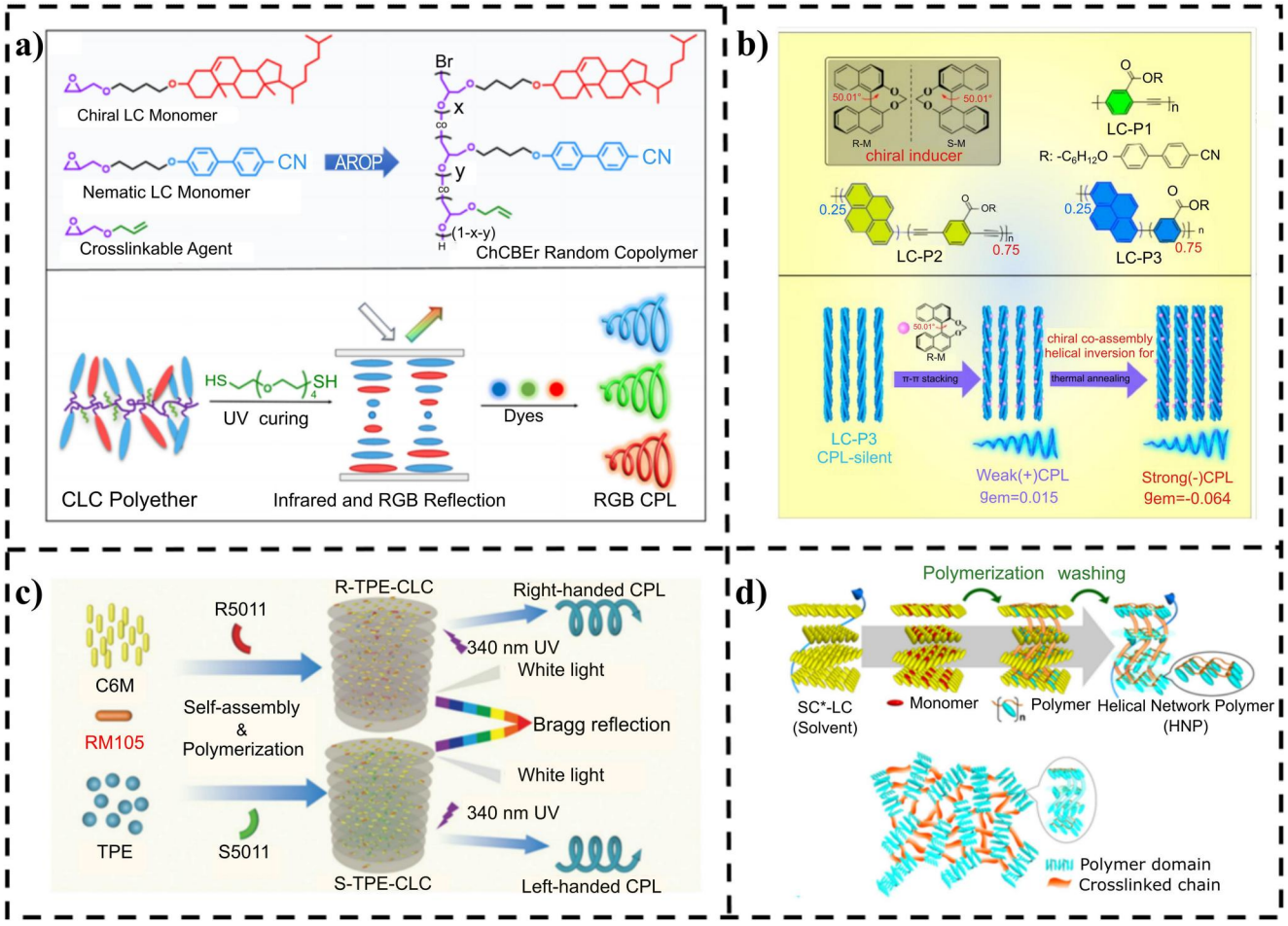

FIGURE 11 (a) Schematic of the dye-doped cholesteric LC elastomers. Reproduced with permission.[91] Copyright 2021, American Chemical Society. (b) Co-assembly route for chiral co-assembly. Reproduced with permission.[203] Copyright 2022, American Chemical Society. (c) Schematic of the formation of structurally colored polymer films with CPL properties. Reproduced with permission.[66] Copyright 2021, The Royal Society of Chemistry. (d) Schematic of the photo-cross-linking polymerization of acrylate derivatives in the Smectic C* LC and network structure of the helical network polymer film. Reproduced with permission.[92] Copyright 2021, American Chemical Society. CPL, circularly polarized luminescent; LC, liquid crystal.

left-handed helical structure. Figure 12a demonstrates the characteristic of the chiral photonic cellulose, which transforms the incident light to the passive CPL and well-controlled handed CPL emission. When the incident light propagating through the films of chiral photonic cellulose, it is converted into the passive L-CPL because of the reflection; however, they transform the passive R-CPL by transmission. Using these cellulose films, the incident light can cover the wavelength from near-UV to near-IR with viewing-side-dependent handedness of passive CPL (Figure 12b,c). Three photonic cellulose films of A shape are demonstrated with different characteristics of PBG (denoted as APBG, Figure 12b, top row). APBG can be seen on a black background by the LCP filter (L-APBG) and RCP filter (R-APBG). The peak wavelengths of the transmission spectra are observed at 640, 565, and 470 nm. The color contrasts of L-APBG, APBG, and R-APBG are consistent and visible. In addition, the R-CPL of photonic cellulose thin films controlled by tuning the PBG and incorporating luminophores opens a novel path for technological advances in the field of CPL materials.

Diffraction gratings as optical components are widely employed in optical multiplexers and signal processors. Lyotropic LC (LLC) are more easily accessible by both natural and synthetic sources than thermotropic LCs; however, it is rarely used in optical gratings. MacLachlan et al.[295] reported optical diffraction gratings with CNC LCs, where hydrogel sheets comprised cholesteric LC structures with the helical axis parallelly aligned to the surface (Figure 13). The homogenous alignment of the cholesteric LCs was obtained by the combination of confining CNCs in a vertical aligned chamber and a magnetic field. Particularly, the mixture containing CNCs and polyacrylamide precursors were filled in the vertically rectangular glass chamber, where phase separation was observed under gravity. Subsequently, the cholesteric LC was aligned using a strong 9.4 T magnetic field, leading to a homogeneous helical axis along the direction of cholesteric LCs. Afterward, the polyacrylamide hydrogel networks were formed near the well-ordered CNCs via UV-irradiation, maintaining the distinct unidirectional LC order and long helical pitch in the liquid state. This

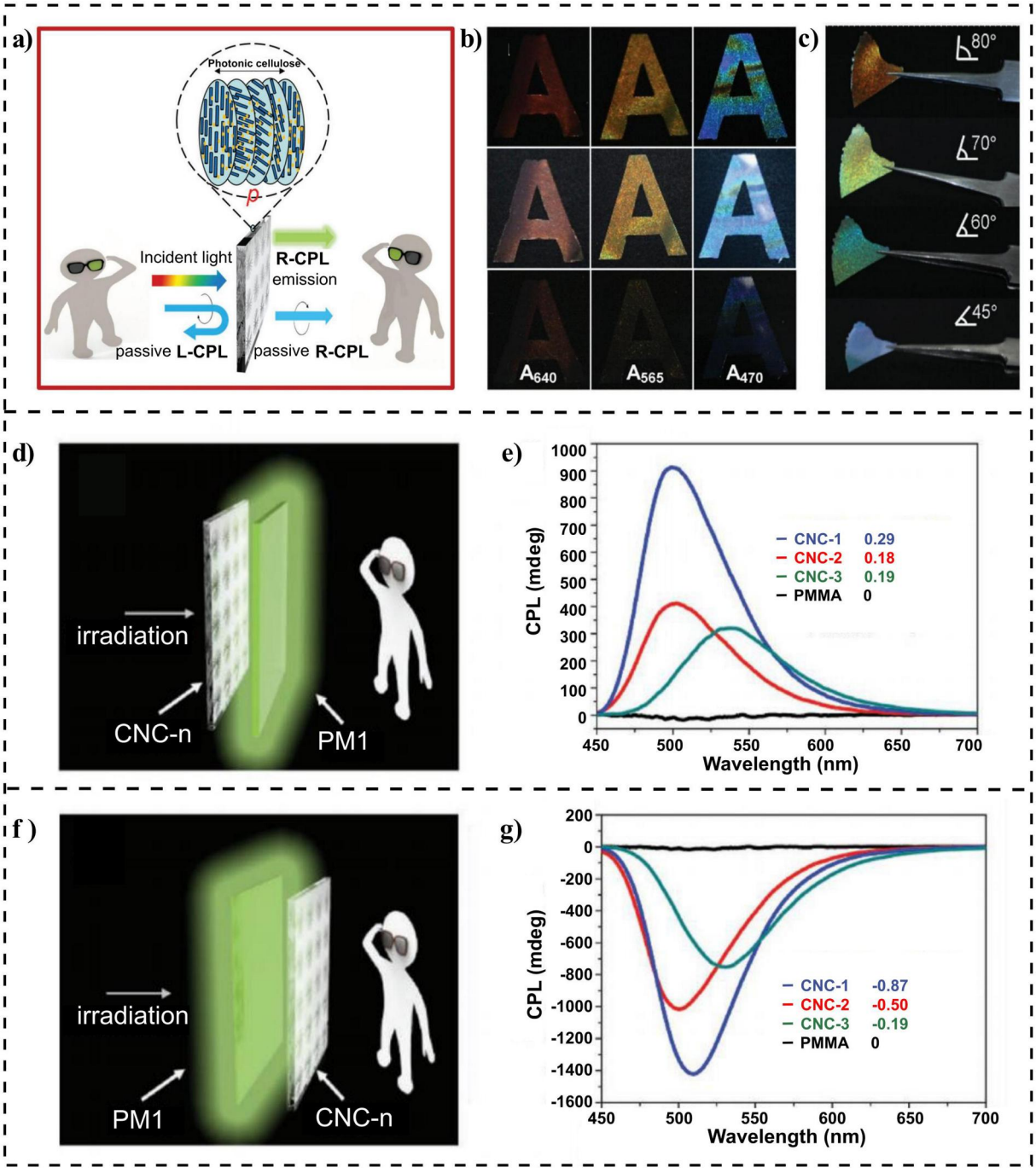

FIGURE 12 (a) CPL of chiral photonic cellulose films. (b) Passive L-CPL and R-CPL enabled by neat chiral photonic cellulose films, CNC-n. (c) Photographs showing angle-dependent iridescence of A640. (d, e) Passive L-CPL for each CNC-n. (f, g) Passive R-CPL for each CNC-n. Reproduced with permission.[65] Copyright 2018, Wiley-VCH. CNC, cellulose nanocrystal; CPL, circularly polarized luminescence.

synthesis approach is able to be widely employed in different grating-based materials, thus creating a new research area of optical materials based on LLCs. The diffracted light depicts the linear polarization rather than the circular polarization (Figure 13b), which appears similar in the diffraction patterns for RCP or LCP (Figure 13b1–b3). This is attributed to the propagation of the incident light, which is perpendicular to the helical axis, thereby prohibiting the Bragg reflection. However, the obvious diffraction effect appears when the polarization of light is parallel to the *x* axis (Figure 13b4) and the color extinction effect occurs if the incident light polarizes parallelly to the *y* axis (Figure 13b6). This method may be capable of being scaled for industrial manufacturing with enhanced performances through fabricating materials, which potentially exhibits a latent foreground of CNC-based optical materials.

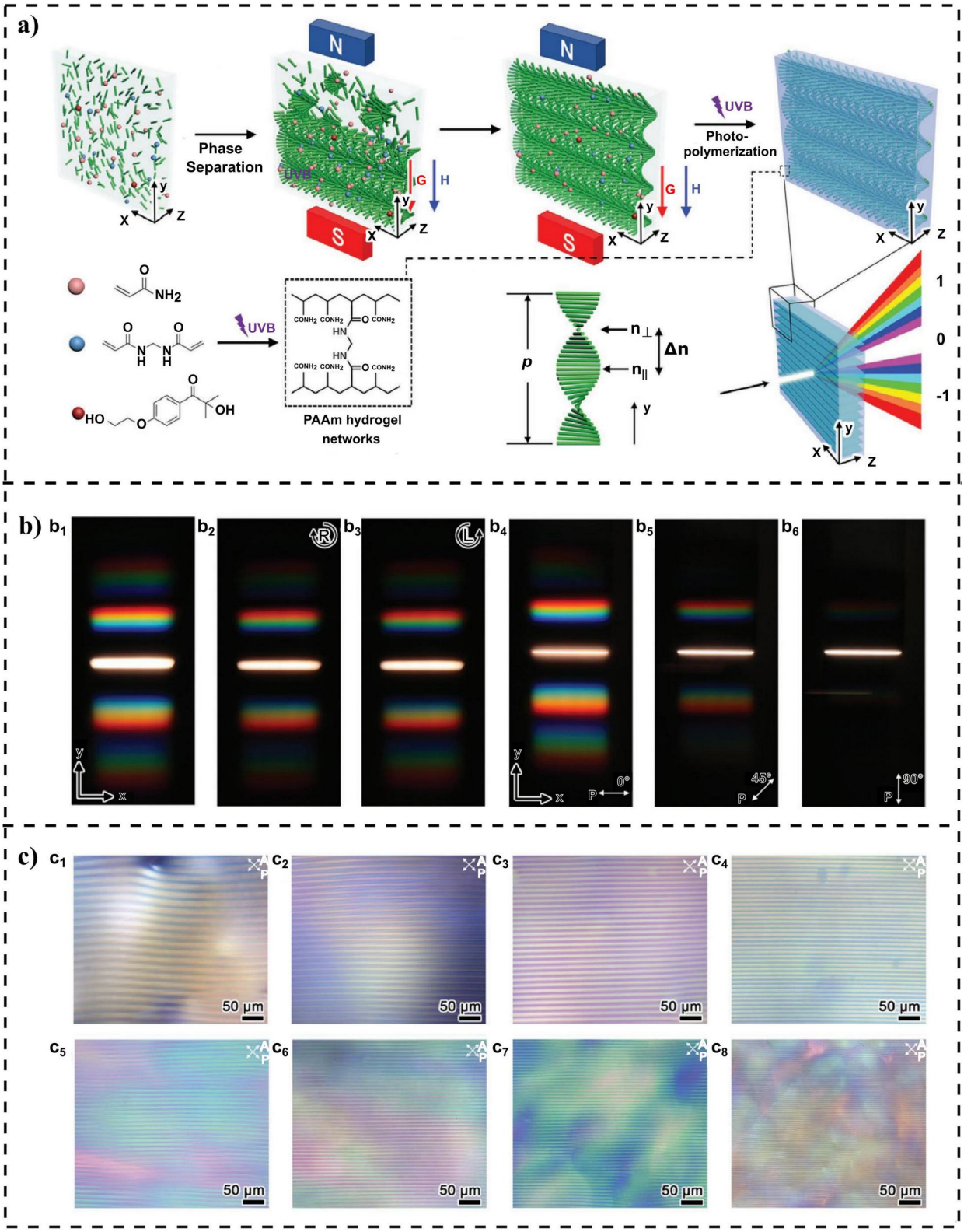

FIGURE 13 (a) Schematic of the optical grating hydrogel. (b) Polarization analyses of the grating. (c) Periodicity control in the various concentrations of CNC in the solution. POM images of the *xy* surface of gratings made from CNC suspensions. Reproduced with permission.[295] Copyright 2018, Wiley-VCH. CNC, cellulose nanocrystals; POM, polarized optical microscope.

7 | CONCLUSIONS AND PERSPECTIVES

Chiral architectures are universal in life and nature, varying at different scales from neutrinos to enantiomers, biomacromolecules, microorganisms, seashells, plants, and galaxies.[12] Chiral orientationally ordered soft matter, such as chiral LCs and LC polymers, are the promising candidates owing to their unique optical and mechanical characteristics with significant potential in the area of chemistry, optics, biology, and materials science. LCs integrate the properties of liquid and crystals from molecular to macroscopic level, thereby offering chances for the essential research on soft matter systems and promoting the development of advanced technology with broad applications. The chiral LCs and LC polymers offer a straightforward pathway in the area of designing of CPL-active functional materials, which are easily accessible and inexpensive in the self-assembly process. This review offers a systematical summary of the emerging progresses on CPL-active chiral LCs and LC polymers. Inspired by the nature beetles of cholesteric architectures, researchers have devoted significant effort to developing various CPL-active chiral LCs and LC polymers, which provide a prospective insight into the fundamental science associated with the functional soft superstructures. Different thermotropic and lyotropic LCs have been used for constructing CPL-active materials with high $|g_{lum}|$. Inorganic nanomaterials, including QDs, nanoparticles, and perovskites, are doped into the predefined handedness cholesteric superstructure stack to obtain the CPL. Particularly, metal halide perovskite semiconductors with excellent optical and electrical properties, such as tunable bandgaps and strong light absorption, are used in the cholesteric LCs with helicoidal (helical) superstructures for fabricating an amplified $|g_{lum}|$ up to 1.6. The perovskite nanoparticle layer is placed between two opposite handed filters, where the cholesteric LC film can change unpolarized light emission into CPL.[87] The incorporation of PAN remarkably improves the stability of perovskite and demonstrates a significantly enhanced $|g_{lum}|$ to 1.9 in the cholesteric LC system.[155] The exploration of CPL-active systems in cholesteric LCs builds up a prospective insight on functional soft superstructures, which are significantly important for future applications, consisting of photonic cellulose films and diffraction gratings. Many emerging nanoscale functional organic materials have been applied in bent-core systems to design novel chiral luminescent nanomaterials with enhanced CPL. These materials can be used in several applications, including biological science, information encryption, optical detectors, and 3D displays.[76,135,296-298] The chirality in achiral bent-core LCs contributes to a better grasp of the origin of the molecular chirality. The HNFs can generate CPL using the self-assembled chiral supernanospace, formed by bent-core molecules with chiral additives, including axially biphenyl derivatives, AIE dyes, and nanoparticles, which offer new approaches for fabricating in CPL-active devices with a high $|g_{lum}|$. The polymeric cholesteric LC superstructures demonstrate highly tunable reflection owing to their elevated processing capacity, enhanced mechanical stability, and structural integrity. The photonic band gap of chiral LC is controllable to obtain a full-color CPL by doping achiral fluorescence dyes. The helical nanofibers formed through the co-assembly of LC polymers and axially chiral binaphthyl derivatives manifest the inverted CPL behavior through intermolecular $\pi-\pi$ stacking interactions.

Despite of the significant and extensive efforts on CPL-active chiral LCs with considerable achievements, the development of CPL-active nanomaterial strategies is still in its infancy. Several challenges need to be solved for the important breakthrough research in the promising area of CPL. A highly challenging task is to develop CPL-active materials with high optical $|g_{lum}|$ approaching the theoretical value of ± 2. The values of $|g_{lum}|$ in most of the cholesteric LC structures are not as high as expected. Therefore, novel mechanisms and new manufacturing technologies are required to design and fabricate new materials. The unique characteristics of inorganic and organic materials, which satisfy the requirement to design CPL-active material with large $|g_{lum}|$, can be integrated into chiral LCs and LC polymers through interdisciplinary research to modify the functions of CPL-based systems. Another challenge is to endow the CPL-active LCs with tunable wavelengths from UV, visible, near-infrared even to the terahertz regions. Though QDs have always been applied to tune the wavelength from visible to near-infrared regions in the organic solvent system, several challenges associated with the LC systems need to be addressed. In addition, substantial endeavor should be focused on investigating more complex and advanced functional devices based on the chiral LCs and LC polymers. Many LC phases, such as 2D chiral smectic and 3D BPs, have potential to be utilized in the advancement of CPL-active LCs with unprecedented functionalities. Potentially, the unique properties of LCs with CPL are speculated to assist in designing the programmable and reconfigurable chiral functional nanomaterials. A bridge is intended to build between the research in CPL-active material and that of diverse applications. Scientists with multidisciplinary research backgrounds could concentrate on the progress of the tissue-like materials, smart textiles, and the wearable flexible displays as well as take the responsibility to bring these CPL-based chiral LCs and LC polymers into technological applications comprising the optical spintronics, optical information processing, quantum communications, and fundamental breakthrough in the advanced chiral functional nanomaterials using the concepts of physics, chemistry, materials science, optics, electronics, display, and other interdisciplinary fields.

AUTHOR CONTRIBUTIONS

Jiao Liu: Writing – original draft (lead). **Zhen-Peng Song**: Software (equal); validation (equal); visualization (equal); writing – original draft (supporting). **Lu-Yao Sun**: Software (equal); visualization (equal); writing – original draft (equal). **Bing-Xiang Li**: Funding acquisition (lead); project

administration (lead). **Yan-Qing Lu**: Project administration (lead). **Quan Li**: Project administration (lead); writing – review & editing (lead).

ACKNOWLEDGMENTS

The work was supported by the National Key Research and Development Program of China (No. 2022YFA1405000), the Natural Science Foundation of Jiangsu Province, Major Project (No. BK20212004), Jiangsu Innovation Team Program, and Natural Science Research Start-up Foundation of Recruiting Talents of Nanjing University of Posts and Telecommunications (No. NY222053).

CONFLICT OF INTEREST STATEMENT

The authors declare no conflict of interest.

ORCID

Bing-Xiang Li https://orcid.org/0000-0003-4727-1572
Yan-Qing Lu https://orcid.org/0000-0001-6151-8557
Quan Li https://orcid.org/0000-0002-9042-360X

REFERENCES

1. Y. Chen, W. Du, Q. Zhang, O. Ávalos-Ovando, J. Wu, Q.-H. Xu, N. Liu, H. Okamoto, A. O. Govorov, Q. Xiong, C.-W. Qiu, *Nat. Rev. Phys.* **2021**, *4*, 113.
2. D. Vila-Liarte, N. A. Kotov, L. M. Liz-Marzan, *Chem. Sci.* **2022**, *13*, 595.
3. F. P. Milton, J. Govan, M. V. Mukhina, Y. K. Gun'ko, *Nanoscale Horiz.* **2016**, *1*, 14.
4. L. D. Barron, *Chem. Soc. Rev.* **1986**, *15*, 189.
5. W. H. De Camp, *Chirality* **1989**, *1*, 97.
6. J. Mun, M. Kim, Y. Yang, T. Badloe, J. Ni, Y. Chen, C.-W. Qiu, J. Rho, *Light Sci. Appl.* **2020**, *9*, 139.
7. W. H. Brooks, W. C. Guida, K. G. Daniel, *Curr. Top. Med. Chem.* **2011**, *11*, 760.
8. A. Nitti, D. Pasini, *Adv. Mater.* **2020**, *32*, e1908021.
9. J. M. Ribó, *Symmetry* **2020**, *12*, 3.
10. K. Ariga, T. Mori, T. Kitao, T. Uemura, *Adv. Mater.* **2020**, *32*, 1905657.
11. S.-H. Yang, R. Naaman, Y. Paltiel, S. S. P. Parkin, *Nat. Rev. Phys.* **2021**, *3*, 328.
12. M. Liu, L. Zhang, T. Wang, *Chem. Rev.* **2015**, *115*, 7304.
13. W. Wu, W. Hu, G. Qian, H. Liao, X. Xu, F. Berto, *Mater. Des.* **2019**, *180*, 107950.
14. W. A. Bonner, *Origins Life Evol. Biospheres* **1995**, *25*, 175.
15. H. Zhang, S. Li, A. Qu, C. Hao, M. Sun, L. Xu, C. Xu, H. Kuang, *Chem. Sci.* **2020**, *11*, 12937.
16. I. Dierking, *Symmetry* **2014**, *6*, 444.
17. P.-T. Chiu, C.-Y. Yang, Z.-H. Xie, M.-Y. Chang, Y.-C. Hung, R.-M. Ho, *Adv. Opt. Mater.* **2021**, *9*, 2002133.
18. V. K. Valev, J. J. Baumberg, C. Sibilia, T. Verbiest, *Adv. Mater.* **2013**, *25*, 2517.
19. Y. Luo, C. Chi, M. Jiang, R. Li, S. Zu, Y. Li, Z. Fang, *Adv. Opt. Mater.* **2017**, *5*, 1700040.
20. X. Zhang, Y. Xu, C. Valenzuela, X. Zhang, L. Wang, W. Feng, Q. Li, *Light Sci. Appl.* **2022**, *11*, 223.
21. M. J. Urban, C. Shen, X.-T. Kong, C. Zhu, A. O. Govorov, Q. Wang, M. Hentschel, N. Liu, *Annu. Rev. Phys. Chem.* **2019**, *70*, 275.
22. Y. Y. Lee, R. M. Kim, S. W. Im, M. Balamurugan, K. T. Nam, *Nanoscale* **2020**, *12*, 58.
23. K. Saito, T. Tatsuma, *Nano Lett.* **2018**, *18*, 3209.
24. Y. Ru, L. Ai, T. Jia, X. Liu, S. Lu, Z. Tang, B. Yang, *Nano Today* **2020**, *34*, 100953.
25. L. Xiao, T. An, L. Wang, X. Xu, H. Sun, *Nano Today* **2020**, *30*, 100824.
26. K. Dietrich, D. Lehr, C. Helgert, A. Tunnermann, E. B. Kley, *Adv. Mater.* **2012**, *24*, OP321.
27. N. A. Kotov, L. M. Liz-Marzán, P. S. Weiss, *ACS Nano* **2021**, *15*, 12457.
28. A. Nemati, L. Querciagrossa, C. Callison, S. Shadpour, T. Mori, D. P. Nunes Gonçalves, X. Cui, R. Ai, J. Wang, C. Zannoni, T. Hegmann, *Sci. Adv.* **2022**, *8*, eabl4385.
29. A. Nemati, S. Shadpour, L. Querciagrossa, L. Li, T. Mori, M. Gao, C. Zannoni, T. Hegmann, *Nat. Commun.* **2018**, *9*, 3908.
30. H.-E. Lee, H.-Y. Ahn, J. Mun, Y. Y. Lee, M. Kim, N. H. Cho, K. Chang, W. S. Kim, J. Rho, K. T. Nam, *Nature* **2018**, *556*, 360.
31. J. Yan, W. Feng, J.-Y. Kim, J. Lu, P. Kumar, Z. Mu, X. Wu, X. Mao, N. A. Kotov, *Chem. Mater.* **2019**, *32*, 476.
32. X. Lan, X. Lu, C. Shen, Y. Ke, W. Ni, Q. Wang, *J. Am. Chem. Soc.* **2015**, *137*, 457.
33. J. Lu, Y. Xue, N. A. Kotov, *Isr. J. Chem.* **2021**, *61*, 851.
34. J. Zhu, F. Wu, Z. Han, Y. Shang, F. Liu, H. Yu, L. Yu, N. Li, B. Ding, *Nano Lett.* **2021**, *21*, 3573.
35. A. Kuzyk, R. Schreiber, H. Zhang, A. O. Govorov, T. Liedl, N. Liu, *Nat. Mater.* **2014**, *13*, 862.
36. Q. Jiang, X. Xu, P.-A. Yin, K. Ma, Y. Zhen, P. Duan, Q. Peng, W.-Q. Chen, B. Ding, *J. Am. Chem. Soc.* **2019**, *141*, 9490.
37. A. D. Merg, J. C. Boatz, A. Mandal, G. Zhao, S. Mokashi-Punekar, C. Liu, X. Wang, P. Zhang, P. C. A. van der Wel, N. L. Rosi, *J. Am. Chem. Soc.* **2016**, *138*, 13655.
38. D. P. N. Gonçalves, M. E. Prévôt, Ş. Üstünel, T. Ogolla, A. Nemati, S. Shadpour, T. Hegmann, *Liq. Cryst. Rev.* **2021**, *9*, 1.
39. L. Wang, A. M. Urbas, Q. Li, *Adv. Mater.* **2020**, *32*, e1801335.
40. J. Uchida, B. Soberats, M. Gupta, T. Kato, *Adv. Mater.* **2022**, *34*, e2109063.
41. H. K. Bisoyi, Q. Li, *Chem. Rev.* **2016**, *116*, 15089.
42. T. Kato, M. Yoshio, T. Ichikawa, B. Soberats, H. Ohno, M. Funahashi, *Nat. Rev. Mater.* **2017**, *2*, 17001.
43. S. Sergeyev, W. Pisula, Y. H. Geerts, *Chem. Soc. Rev.* **2007**, *36*, 1902.
44. N. Tamaoki, *Adv. Mater.* **2001**, *13*, 1135.
45. M. Wang, C. Zou, J. Sun, L. Zhang, L. Wang, J. Xiao, F. Li, P. Song, H. Yang, *Adv. Funct. Mater.* **2017**, *27*, 1702261.
46. W. Hu, L. Wang, M. Wang, T. Zhong, Q. Wang, L. Zhang, F. Chen, K. Li, Z. Miao, D. Yang, H. Yang, *Nat. Commun.* **2021**, *12*, 1440.
47. L. Wang, Q. Li, *Adv. Funct. Mater.* **2016**, *26*, 10.
48. T.-H. Lin, Y. Li, C.-T. Wang, H.-C. Jau, C.-W. Chen, C.-C. Li, H. K. Bisoyi, T. J. Bunning, Q. Li, *Adv. Mater.* **2013**, *25*, 5050.
49. H. Kikuchi, M. Yokota, Y. Hisakado, H. Yang, T. Kajiyama, *Nat. Mater.* **2002**, *1*, 64.
50. D. Grzelak, P. Szustakiewicz, C. Tollan, S. Raj, P. Kral, W. Lewandowski, L. M. Liz-Marzan, *J. Am. Chem. Soc.* **2020**, *142*, 18814.
51. M. Baginski, M. Tupikowska, G. Gonzalez-Rubio, M. Wojcik, W. Lewandowski, *Adv. Mater.* **2020**, *32*, e1904581.
52. J. J. Lee, B. C. Kim, H. J. Choi, S. Bae, F. Araoka, S. W. Choi, *ACS Nano* **2020**, *14*, 5243.
53. P. Lesiak, K. Bednarska, W. Lewandowski, M. Wojcik, S. Polakiewicz, M. Baginski, T. Osuch, K. Markowski, K. Orzechowski, M. Makowski, J. Bolek, T. R. Wolinski, *ACS Nano* **2019**, *13*, 10154.
54. W. Lewandowski, N. Vaupotic, D. Pociecha, E. Gorecka, L. M. Liz-Marzan, *Adv. Mater.* **2020**, *32*, e1905591.
55. W. Park, T. Ha, T.-T. Kim, A. Zep, H. Ahn, T. J. Shin, K. I. Sim, T. S. Jung, J. H. Kim, D. Pociecha, E. Gorecka, D. K. Yoon, *NPG Asia Mater.* **2019**, *11*, 1.
56. S. Maniappan, A. B. Jadhav, J. Kumar, *Front. Chem.* **2020**, *8*, 557650.
57. R. Dreher, G. Meier, A. Saupe, *Mol. Cryst. Liq. Cryst.* **2007**, *13*, 17.
58. M. Nakata, D. R. Link, F. Araoka, J. Thisayukta, Y. Takanishi, K. Ishikawa, J. Watanabe, H. Takezoe, *Liq. Cryst.* **2010**, *28*, 1301.

59. M. Xu, C. Ma, J. Zhou, Y. Liu, X. Wu, S. Luo, W. Li, H. Yu, Y. Wang, Z. Chen, J. Li, S. Liu, *J. Mater. Chem. C* **2019**, *7*, 13794.
60. D. M. Lee, J. W. Song, Y. J. Lee, C. J. Yu, J. H. Kim, *Adv. Mater.* **2017**, *29*, 1705692.
61. J. Gong, X. Zhang, *Coord. Chem. Rev.* **2022**, *453*, 214329.
62. J. R. Brandt, X. Wang, Y. Yang, A. J. Campbell, M. J. Fuchter, *J. Am. Chem. Soc.* **2016**, *138*, 9743.
63. F. Song, Z. Zhao, Z. Liu, J. W. Y. Lam, B. Z. Tang, *J. Mater. Chem. C* **2020**, *8*, 3284.
64. S. Koga, S. Ueki, M. Shimada, R. Ishii, Y. Kurihara, Y. Yamanoi, J. Yuasa, T. Kawai, T. A. Uchida, M. Iwamura, K. Nozaki, H. Nishihara, *J. Org. Chem.* **2017**, *82*, 6108.
65. H. Zheng, W. Li, W. Li, X. Wang, Z. Tang, S. X. Zhang, Y. Xu, *Adv. Mater.* **2018**, *30*, e1705948.
66. B. Ni, Y. Li, W. Liu, B. Li, H. Li, Y. Yang, *Chem. Commun.* **2021**, *57*, 2796.
67. X. Jin, Y. Sang, Y. Shi, Y. Li, X. Zhu, P. Duan, M. Liu, *ACS Nano* **2019**, *13*, 2804.
68. J. Han, S. Guo, H. Lu, S. Liu, Q. Zhao, W. Huang, *Adv. Opt. Mater.* **2018**, *6*, 1800538.
69. Y. Sang, D. Yang, Z. Shen, P. Duan, M. Liu, *J. Ind. Eng. Chem.* **2020**, *124*, 17274.
70. K. Dhbaibi, L. Abella, S. Meunier-Della-Gatta, T. Roisnel, N. Vanthuyne, B. Jamoussi, G. Pieters, B. Racine, E. Quesnel, J. Autschbach, J. Crassous, L. Favereau, *Chem. Sci.* **2021**, *12*, 5522.
71. Y. He, S. Lin, J. Guo, Q. Li, *Aggregate* **2021**, *2*, e141.
72. S. Liu, Y. Chen, W. Xu, Q. Zhao, W. Huang, *Macromol. Rapid Commun.* **2012**, *33*, 461.
73. G. Muller, *Dalton Trans.* **2009**, 9692.
74. K. Takaishi, K. Iwachido, T. Ema, *J. Am. Chem. Soc.* **2020**, *142*, 1774.
75. L. Wang, L. Yin, W. Zhang, X. Zhu, M. Fujiki, *J. Am. Chem. Soc.* **2017**, *139*, 13218.
76. Y. Yang, R. C. da Costa, M. J. Fuchter, A. J. Campbell, *Nat. Photonics* **2013**, *7*, 634.
77. J. C. Weaver, G. W. Milliron, A. Miserez, K. Evans-Lutterodt, S. Herrera, I. Gallana, W. J. Mershon, P. Zavattieri, E. DiMasi, D. Kisailus, *Science* **2012**, *44*, 9692.
78. I. M. Daly, M. J. How, J. C. Partridge, S. E. Temple, N. J. Marshall, T. W. Cronin, N. W. Roberts, *Nat. Commun.* **2016**, *7*, 12140.
79. S. Vignolini, P. J. Rudall, A. V. Rowland, A. Reed, E. Moyroud, R. B. Faden, J. J. Baumberg, B. J. Glover, U. Steiner, *Proc. Natl. Acad. Sci. U. S. A.* **2012**, *109*, 15712.
80. A. Matranga, S. Baig, J. Boland, C. Newton, T. Taphouse, G. Wells, S. Kitson, *Adv. Mater.* **2013**, *25*, 520.
81. W. Li, Z. J. Coppens, L. V. Besteiro, W. Wang, A. O. Govorov, J. Valentine, *Nat. Commun.* **2015**, *6*, 8379.
82. J. Hwang, M. H. Song, B. Park, S. Nishimura, T. Toyooka, J. W. Wu, Y. Takanishi, K. Ishikawa, H. Takezoe, *Nat. Mater.* **2005**, *4*, 383.
83. J. T. Collins, C. Kuppe, D. C. Hooper, C. Sibilia, M. Centini, V. K. Valev, *Adv. Opt. Mater.* **2017**, *5*, 1700182.
84. Y. Deng, M. Wang, Y. Zhuang, S. Liu, W. Huang, Q. Zhao, *Light Sci. Appl.* **2021**, *10*, 76.
85. Y. Wang, J. Shi, J. Chen, W. Zhu, E. Baranoff, *J. Mater. Chem. C* **2015**, *3*, 7993.
86. X. Yang, X. Jin, T. Zhao, P. Duan, *Mater. Chem. Front.* **2021**, *5*, 4821.
87. C.-T. Wang, K. Chen, P. Xu, F. Yeung, H.-S. Kwok, G. Li, *Adv. Funct. Mater.* **2019**, *29*, 1903155.
88. D. Han, X. Yang, J. Han, J. Zhou, T. Jiao, P. Duan, *Nat. Commun.* **2020**, *11*, 5659.
89. J. Liu, Y. Molard, M. E. Prevot, T. Hegmann, *ACS Appl. Mater. Interfaces* **2022**, *14*, 29398.
90. B. A. San Jose, S. Matsushita, K. Akagi, *J. Am. Chem. Soc.* **2012**, *134*, 19795.
91. W. Wei, M. A. Farooq, H. Xiong, *Langmuir* **2021**, *37*, 11922.
92. H. Yamamoto, T. Inagaki, J. Park, S. Yoshida, K. Kaneko, T. Hanasaki, K. Akagi, *Macromolecules* **2021**, *54*, 8977.
93. Y. Sang, J. Han, T. Zhao, P. Duan, M. Liu, *Adv. Mater.* **2020**, *32*, e1900110.
94. J. Y. Kim, J. Yeom, G. Zhao, H. Calcaterra, J. Munn, P. Zhang, N. Kotov, *J. Am. Chem. Soc.* **2019**, *141*, 11739.
95. F. Zinna, M. Pasini, F. Galeotti, C. Botta, L. Di Bari, U. Giovanella, *Adv. Funct. Mater.* **2017**, *27*, 1603719.
96. Z. Liu, J. Ai, P. Kumar, E. You, X. Zhou, X. Liu, Z. Tian, P. Bour, Y. Duan, L. Han, N. A. Kotov, S. Ding, S. Che, *Angew. Chem. Int. Ed.* **2020**, *59*, 15226.
97. P.-C. Lin, S. Lin, P. C. Wang, R. Sridhar, *Biotechnol. Adv.* **2014**, *32*, 711.
98. M. Schulz, J. Zablocki, O. S. Abdullaeva, S. Bruck, F. Balzer, A. Lutzen, O. Arteaga, M. Schiek, *Nat. Commun.* **2018**, *9*, 2413.
99. A. H. G. David, R. Casares, J. M. Cuerva, A. G. Campana, V. Blanco, *J. Am. Chem. Soc.* **2019**, *141*, 18064.
100. X.-M. Chen, S. Zhang, X. Chen, Q. Li, *ChemPhotoChem* **2022**, *6*, e202100256.
101. S. Huo, P. Duan, T. Jiao, Q. Peng, M. Liu, *Angew. Chem. Int. Ed.* **2017**, *56*, 12174.
102. M. Xu, X. Wu, Y. Yang, C. Ma, W. Li, H. Yu, Z. Chen, J. Li, K. Zhang, S. Liu, *ACS Nano* **2020**, *14*, 11130.
103. Y. Nagata, T. Nishikawa, M. Suginome, *Chem. Commun.* **2014**, *50*, 9951.
104. E. M. Sanchez-Carnerero, F. Moreno, B. L. Maroto, A. R. Agarrabeitia, M. J. Ortiz, B. G. Vo, G. Muller, S. de la Moya, *J. Am. Chem. Soc.* **2014**, *136*, 3346.
105. X. Shang, I. Song, H. Ohtsu, Y. H. Lee, T. Zhao, T. Kojima, J. H. Jung, M. Kawano, J. H. Oh, *Adv. Mater.* **2017**, *29*, 1605828.
106. Q. Zhao, C. Huang, F. Li, *Chem. Soc. Rev.* **2010**, *40*, 2508.
107. Q. Zhao, F. Li, C. Huang, *Chem. Soc. Rev.* **2009**, *39*, 3007.
108. Y. Zhuang, S. Guo, Y. Deng, S. Liu, Q. Zhao, *Chem. Asian J.* **2019**, *14*, 3791.
109. Y. H. Kim, Y. Zhai, E. A. Gaulding, S. N. Habisreutinger, T. Moot, B. A. Rosales, H. Lu, A. Hazarika, R. Brunecky, L. M. Wheeler, J. J. Berry, M. C. Beard, J. M. Luther, *ACS Nano* **2020**, *14*, 8816.
110. Y. Gao, C. Ren, X. Lin, T. He, *Front. Chem.* **2020**, *8*, 458.
111. Y. Chen, P. Lu, Z. Li, Y. Yuan, Q. Ye, H. Zhang, *ACS Appl. Mater. Interfaces* **2020**, *12*, 56604.
112. K. Yao, Y. Shen, Y. Li, X. Li, Y. Quan, Y. Cheng, *J. Phys. Chem. Lett.* **2021**, *12*, 598.
113. J. Han, P. Duan, X. Li, M. Liu, *J. Am. Chem. Soc.* **2017**, *139*, 9783.
114. M. Mitov, *Adv. Mater.* **2012**, *24*, 6260.
115. N. Lu, X. Gao, M. Pan, B. Zhao, J. Deng, *Macromolecules* **2020**, *53*, 8041.
116. F. Wang, W. Ji, P. Yang, C.-L. Feng, *ACS Nano* **2019**, *13*, 7281.
117. X. Yang, X. Lin, Y. Zhao, Y. S. Zhao, D. Yan, *Angew. Chem. Int. Ed.* **2017**, *56*, 7853.
118. J. Zhang, Q. Liu, W. Wu, J. Peng, H. Zhang, F. Song, B. He, X. Wang, H. H. Sung, M. Chen, B. S. Li, S. H. Liu, J. W. Y. Lam, B. Z. Tang, *ACS Nano* **2019**, *13*, 3618.
119. L. E. Hough, H. T. Jung, D. Krüerke, M. S. Heberling, M. Nakata, C. D. Jones, D. Chen, D. R. Link, J. Zasadzinski, G. Heppke, J. P. Rabe, W. Stocker, E. Körblova, D. M. Walba, M. A. Glaser, N. A. Clark, *Science* **2009**, *325*, 456.
120. E. Tsai, J. M. Richardson, E. Korblova, M. Nakata, D. Chen, Y. Shen, R. Shao, N. A. Clark, D. M. Walba, *Angew. Chem. Int. Ed.* **2013**, *52*, 5254.
121. T. Kato, J. Uchida, T. Ichikawa, T. Sakamoto, *Angew. Chem. Int. Ed.* **2018**, *57*, 4355.
122. H. K. Bisoyi, Q. Li, *Chem. Rev.* **2022**, *122*, 4887.
123. H. K. Bisoyi, Q. Li, *Acc. Chem. Res.* **2014**, *47*, 3184.
124. S. Tokunaga, Y. Itoh, Y. Yaguchi, H. Tanaka, F. Araoka, H. Takezoe, T. Aida, *Adv. Mater.* **2016**, *28*, 4077.
125. C. D. Edgar, D. G. Gray, *Cellulose* **2001**, *8*, 5.

126. A. Ryabchun, A. Bobrovsky, *Adv. Opt. Mater.* **2018**, *6*, 1800335.
127. L. Zhu, C.-T. Xu, P. Chen, Y.-H. Zhang, S.-J. Liu, Q. M. Chen, S.-J. Ge, W. Hu, Y.-Q. Lu, *Light Sci. Appl.* **2022**, *11*, 135.
128. W. D. St John, W. J. Fritz, Z. J. Lu, D. Yang, *Phys. Rev. E* **1995**, *51*, 1191.
129. J. Xiang, Y. Li, Q. Li, D. A. Paterson, J. M. D. Storey, C. T. Imrie, O. D. Lavrentovich, *Adv. Mater.* **2015**, *27*, 3014.
130. L.-L. Ma, C.-Y. Li, J.-T. Pan, Y.-E. Ji, C. Jiang, R. Zheng, Z.-Y. Wang, Y. Wang, B.-X. Li, Y.-Q. Lu, *Light Sci. Appl.* **2022**, *11*, 270.
131. R. Dreher, G. Meier, *Phys. Rev. A* **1973**, *8*, 1616.
132. Y. Yang, L. Wang, H. Yang, Q. Li, *Small Sci.* **2021**, *1*, 2100007.
133. P. Chen, L.-L. Ma, W. Hu, Z.-X. Shen, H. K. Bisoyi, S.-B. Wu, S.-J. Ge, Q. Li, Y.-Q. Lu, *Nat. Commun.* **2019**, *10*, 2518.
134. L. Ma, C. Li, L. Sun, Z. Song, Y. Lu, B. Li, *Photonics Res.* **2022**, *10*, 786.
135. X. Zhan, F.-F. Xu, Z. Zhou, Y. Yan, J. Yao, Y. S. Zhao, *Adv. Mater.* **2021**, *33*, e2104418.
136. H. K. Bisoyi, T. J. Bunning, Q. Li, *Adv. Mater.* **2018**, *30*, e1706512.
137. L. Zhang, L. Wang, U. S. Hiremath, H. K. Bisoyi, G. G. Nair, C. V. Yelamaggad, A. M. Urbas, T. J. Bunning, Q. Li, *Adv. Mater.* **2017**, *29*, 1700676.
138. Z.-G. Zheng, Y. Li, H. K. Bisoyi, L. Wang, T. J. Bunning, Q. Li, *Nature* **2016**, *531*, 352.
139. L. Ma, C. Liu, S. Wu, P. Chen, Q. Chen, J. Qian, S. Ge, Y. Wu, W. Hu, Y. Lu, *Sci. Adv.* **2021**, *7*, eabh3505.
140. *Liquid Crystals beyond Displays* (Ed: Q. Li), Wiley, Hoboken, NJ, USA **2012**.
141. J. Li, H. K. Bisoyi, J. Tian, J. Guo, Q. Li, *Adv. Mater.* **2019**, *31*, 1807751.
142. C. A. Emeis, L. J. Oosterhoff, *Chem. Phys. Lett.* **1967**, *1*, 129.
143. J. L. Lunkley, D. Shirotani, K. Yamanari, S. Kaizaki, G. Mulle, *J. Am. Chem. Soc.* **2008**, *130*, 13814.
144. F. Zinna, L. Di Bari, *Chirality* **2015**, *27*, 1.
145. R. Carr, N. H. Evans, D. Parker, *Chem. Soc. Rev.* **2012**, *41*, 7673.
146. J. Chen, X. Gao, Q. Zheng, J. Liu, D. Meng, H. Li, R. Cai, H. Fan, Y. Ji, X. Wu, *ACS Nano* **2021**, *15*, 15114.
147. Y. Shi, P. Duan, S. Huo, Y. Li, M. Liu, *Adv. Mater.* **2018**, *30*, e1705011.
148. U. Tohgha, K. K. Deol, A. G. Porter, S. G. Bartko, J. K. Choi, B. M. Leonard, K. Varga, J. Kubelka, G. Muller, M. Balaz, *ACS Nano* **2013**, *7*, 11094.
149. J. Kumar, T. Kawai, T. Nakashima, *Chem. Commun.* **2017**, *53*, 1269.
150. M. Naito, K. Iwahori, A. Miura, M. Yamane, I. Yamashita, *Angew. Chem. Int. Ed.* **2010**, *49*, 7006.
151. J. Ahn, E. Lee, J. Tan, W. Yang, B. Kim, J. Moon, *Mater. Horiz.* **2017**, *4*, 851.
152. S. Jiang, N. A. Kotov, *Adv. Mater.* **2022**, e2108431.
153. D. B. Mitzi, *Chem. Rev.* **2019**, *119*, 3033.
154. D. Han, C. Li, C. Jiang, X. Jin, X. Wang, R. Chen, J. Cheng, P. Duan, *Aggregate* **2021**, *3*, e148.
155. S. Liu, X. Liu, Y. Wu, D. Zhang, Y. Wu, H. Tian, Z. Zheng, W.-H. Zhu, *Matter* **2022**, *5*, 2319.
156. X. Cheng, D. Tu, W. Zheng, X. Chen, *Chem. Commun.* **2020**, *56*, 15118.
157. J. Zhou, Q. Liu, W. Feng, Y. Sun, F. Li, *Chem. Rev.* **2015**, *115*, 395.
158. T.-A. Lin, C. F. Perkinson, M. A. Baldo, *Adv. Mater.* **2020**, *32*, e1908175.
159. X. Li, F. Zhang, D. Zhao, *Chem. Soc. Rev.* **2015**, *44*, 1346.
160. B. Chen, F. Wang, *Trends Chem.* **2020**, *2*, 427.
161. S. Han, R. Deng, X. Xie, X. Liu, *Angew. Chem. Int. Ed.* **2014**, *53*, 11702.
162. S. Wu, H. J. Butt, *Adv. Mater.* **2016**, *28*, 1208.
163. Y. Wang, S. Song, S. Zhang, H. Zhang, *Nano Today* **2019**, *25*, 38.
164. Z. Zhang, Y. Chen, Y. Zhang, *Small* **2022**, *18*, e2103241.
165. L. Wang, H. Dong, Y. Li, R. Liu, Y.-F. Wang, H. K. Bisoyi, L.-D. Sun, C.-H. Yan, Q. Li, *Adv. Mater.* **2015**, *27*, 2065.
166. C. Li, P. Duan, *Chem. Lett.* **2021**, *50*, 546.
167. Y. Wei, Z. Cheng, J. Lin, *Chem. Soc. Rev.* **2019**, *48*, 310.
168. S. Liang, M. Zhang, G. M. Biesold, W. Choi, Y. He, Z. Li, D. Shen, Z. Lin, *Adv. Mater.* **2021**, *33*, e2005888.
169. H. Dong, S.-R. Du, X.-Y. Zheng, G.-M. Lyu, L.-D. Sun, L.-D. Li, P.-Z. Zhang, C. Zhang, C.-H. Yan, *Chem. Rev.* **2015**, *115*, 10725.
170. S. De Camillis, P. Ren, Y. Cao, M. Ploschner, D. Denkova, X. Zheng, Y. Lu, J. A. Piper, *Nanoscale* **2020**, *12*, 20347.
171. Y. Zhang, X. Zhu, Y. Zhang, *ACS Nano* **2021**, *15*, 3709.
172. X. Yang, M. Zhou, Y. Wang, P. Duan, *Adv. Mater.* **2020**, *32*, e2000820.
173. X. Gao, X. Qin, X. Yang, Y. Li, P. Duan, *Chem. Commun.* **2019**, *55*, 5914.
174. J. Kumar, T. Nakashima, T. Kawai, *J. Phys. Chem. Lett.* **2015**, *6*, 3445.
175. E. M. Sánchez-Carnerero, A. R. Agarrabeitia, F. Moreno, B. L. Maroto, G. Muller, M. J. Ortiz, S. de la Moya, *Chem. Eur. J.* **2015**, *21*, 13488.
176. K. Matsumoto, Y. Toubaru, S. Tachikawa, A. Miki, K. Sakai, S. Koroki, T. Hirokane, M. Shindo, M. Yoshida, *J. Org. Chem.* **2020**, *85*, 15154.
177. E. Yashima, N. Ousaka, D. Taura, K. Shimomura, T. Ikai, K. Maeda, *Chem. Rev.* **2016**, *116*, 13752.
178. Z.-L. Gong, X. Zhu, Z. Zhou, S.-W. Zhang, D. Yang, B. Zhao, Y.-P. Zhang, J. Deng, Y. Cheng, Y.-X. Zheng, S.-Q. Zang, H. Kuang, P. Duan, M. Yuan, C.-F. Chen, Y. S. Zhao, Y.-W. Zhong, B. Z. Tang, M. Liu, *Sci. China Chem.* **2021**, *64*, 2060.
179. S. J. D. Lugger, S. J. A. Houben, Y. Foelen, M. G. Debije, A. Schenning, D. J. Mulder, *Chem. Rev.* **2022**, *122*, 4946.
180. J. Sol, H. Sentjens, L. Yang, N. Grossiord, A. Schenning, M. G. Debije, *Adv. Mater.* **2021**, *33*, e2103309.
181. H. K. Bisoyi, Q. Li, *Angew. Chem. Int. Ed.* **2016**, *55*, 2994.
182. J. Bao, R. Lan, C. Shen, R. Huang, Z. Wang, W. Hu, L. Zhang, H. Yang, *Adv. Opt. Mater.* **2021**, *10*, 2101910.
183. K. V. Le, H. Takezoe, F. Araoka, *Adv. Mater.* **2017**, *29*, 1602737.
184. L. Tran, M. O. Lavrentovich, D. A. Beller, N. Li, K. J. Stebe, R. D. Kamien, *Proc. Natl. Acad. Sci. U. S. A.* **2016**, *113*, 7106.
185. D. K. Yoon, Y. Yi, Y. Shen, E. D. Korblova, D. M. Walba, I. I. Smalyukh, N. A. Clark, *Adv. Mater.* **2011**, *23*, 1962.
186. H. Kim, S. Lee, T. J. Shin, Y. J. Cha, E. Korblova, D. M. Walba, N. A. Clark, S. B. Lee, D. K. Yoon, *Soft Matter* **2013**, *9*, 6185.
187. S. Lee, H. Kim, T. J. Shin, E. Tsai, J. M. Richardson, E. Korblova, D. M. Walba, N. A. Clark, S. B. Lee, D. K. Yoon, *Soft Matter* **2015**, *11*, 3653.
188. S. H. Ryu, H. Kim, S. Lee, Y. J. Cha, T. J. Shin, H. Ahn, E. Korblova, D. M. Walba, N. A. Clark, S. B. Lee, D. K. Yoon, *Soft Matter* **2015**, *11*, 7778.
189. M. J. Gim, H. Kim, D. Chen, Y. Shen, Y. Yi, E. Korblova, D. M. Walba, N. A. Clark, D. K. Yoon, *Sci. Rep.* **2016**, *6*, 29111.
190. D. Chen, J. E. Maclennan, R. Shao, D. K. Yoon, H. Wang, E. Korblova, D. M. Walba, M. A. Glaser, N. A. Clark, *J. Am. Chem. Soc.* **2011**, *133*, 12656.
191. J. Matraszek, N. Topnani, N. Vaupotic, H. Takezoe, J. Mieczkowski, D. Pociecha, E. Gorecka, *Angew. Chem. Int. Ed.* **2016**, *55*, 3468.
192. C. Zhu, C. Wang, A. Young, F. Liu, I. Gunkel, D. Chen, D. Walba, J. Maclennan, N. Clark, A. Hexemer, *Nano Lett.* **2015**, *15*, 3420.
193. K. Kim, H. Kim, S. Y. Jo, F. Araoka, D. K. Yoon, S. W. Choi, *ACS Appl. Mater. Interfaces* **2015**, *7*, 22686.
194. W. Park, J. M. Wolska, D. Pociecha, E. Gorecka, D. K. Yoon, *Adv. Opt. Mater.* **2019**, *7*, 1901399.
195. B. C. Kim, H. J. Choi, J. J. Lee, F. Araoka, S. W. Choi, *Adv. Funct. Mater.* **2019**, *29*, 1903246.
196. S. Shadpour, A. Nemati, J. Liu, T. Hegmann, *ACS Appl. Mater. Interfaces* **2020**, *12*, 13456.
197. C. Duan, Z. Cheng, B. Wang, J. Zeng, J. Xu, J. Li, W. Gao, K. Chen, *Small* **2021**, *17*, e2007306.
198. J. Liu, S. Shadpour, M. E. Prevot, M. Chirgwin, A. Nemati, E. Hegmann, R. P. Lemieux, T. Hegmann, *ACS Nano* **2021**, *15*, 7249.
199. C. Zhang, N. Diorio, O. D. Lavrentovich, A. Jakli, *Nat. Commun.* **2014**, *5*, 3302.

200. C. Zhu, D. Chen, Y. Shen, C. D. Jones, M. A. Glaser, J. E. Maclennan, N. A. Clark, *Phys. Rev. E* **2010**, *81*, 011704.
201. B.-X. Li, R.-L. Xiao, S. V. Shiyanovskii, O. D. Lavrentovich, *Phys. Rev. Res.* **2020**, *2*, 013178.
202. B.-X. Li, V. Borshch, R.-L. Xiao, S. Paladugu, T. Turiv, S. V. Shiyanovskii, O. D. Lavrentovich, *Nat. Commun.* **2018**, *9*, 2912.
203. Y. Zhang, H. Li, Z. Geng, W.-H. Zheng, Y. Quan, Y. Cheng, *ACS Nano* **2022**, *16*, 3173.
204. T. Ikai, M. Okubo, Y. Wada, *J. Am. Chem. Soc.* **2020**, *6*, 1.
205. L. Li, M. Salamonczyk, A. Jakli, T. Hegmann, *Small* **2016**, *12*, 3944.
206. L. Li, M. Salamonczyk, S. Shadpour, C. Zhu, A. Jakli, T. Hegmann, *Nat. Commun.* **2018**, *9*, 714.
207. J. Luo, Z. Xie, J. W. Lam, L. Cheng, H. Chen, C. Qiu, H. S. Kwok, X. Zhan, Y. Liu, D. Zhu, B. Z. Tang, *Chem. Commun.* **2001**, *21*, 1740.
208. J. Han, J. You, X. Li, P. Duan, M. Liu, *Adv. Mater.* **2017**, *29*, 9783.
209. T. Ikeda, M. Takayama, J. Kumar, T. Kawai, T. Haino, *Dalton Trans.* **2015**, *44*, 13156.
210. J.-B. Xiong, H.-T. Feng, J.-P. Sun, W.-Z. Xie, D. Yang, M. Liu, Y.-S. Zheng, *J. Am. Chem. Soc.* **2016**, *138*, 11469.
211. S. Zhang, Y. Sheng, G. Wei, Y. Quan, Y. Cheng, C. Zhu, *Polym. Chem.* **2015**, *6*, 2416.
212. Q. Xia, L. Meng, T. He, G. Huang, B. S. Li, B. Z. Tang, *ACS Nano* **2021**, *15*, 4956.
213. C. Zhang, S. Li, X.-Y. Dong, S.-Q. Zang, *Aggregate* **2021**, *2*, e48.
214. J. Roose, B. Z. Tang, K. S. Wong, *Small* **2016**, *12*, 6495.
215. Y. Hong, J. W. Lam, B. Z. Tang, *Chem. Soc. Rev.* **2011**, *40*, 5361.
216. D. Zhao, F. Fan, J. Cheng, Y. Zhang, K. S. Wong, V. G. Chigrinov, H. S. Kwok, L. Guo, B. Z. Tang, *Adv. Opt. Mater.* **2015**, *3*, 199.
217. J. Mei, N. L. C. Leung, R. T. K. Kwok, J. W. Y. Lam, B. Z. Tang, *Chem. Rev.* **2015**, *115*, 11718.
218. Y. Hong, J. W. Y. Lam, B. Z. Tang, *Chem. Comm.* **2009**, *45*, 4332.
219. J. Li, J. Wang, H. Li, N. Song, D. Wang, B. Z. Tang, *Chem. Soc. Rev.* **2020**, *49*, 1144.
220. S. Lee, H. Kim, E. Tsai, J. M. Richardson, E. Korblova, D. M. Walba, N. A. Clark, S. B. Lee, D. K. Yoon, *Langmuir* **2015**, *31*, 8156.
221. Z.-W. Luo, L. Tao, C.-L. Zhong, Z.-X. Li, K. Lan, Y. Feng, P. Wang, H.-L. Xie, *Macromolecules* **2020**, *53*, 9758.
222. X. Li, W. Hu, Y. Wang, Y. Quan, Y. Cheng, *Chem. Commun.* **2019**, *55*, 5179.
223. X. Li, Q. Li, Y. Wang, Y. Quan, D. Chen, Y. Cheng, *Chemistry* **2018**, *24*, 12607.
224. Y. Wu, L. H. You, Z.-Q. Yu, J.-H. Wang, Z. Meng, Y. Liu, X.-S. Li, K. Fu, X.-K. Ren, B. Z. Tang, *ACS Mater. Lett.* **2020**, *2*, 505.
225. D. Zhao, H. He, X. Gu, L. Guo, K. S. Wong, J. W. Y. Lam, B. Z. Tang, *Adv. Opt. Mater.* **2016**, *4*, 534.
226. M. Mitov, C. Portet, C. Bourgerette, E. Snoeck, M. Verelst, *Nat. Mater.* **2002**, *1*, 229.
227. L. Wang, W. He, X. Xiao, F. Meng, Y. Zhang, P. Yang, L. Wang, J. Xiao, H. Yang, Y. Lu, *Small* **2012**, *8*, 2189.
228. K. Zhou, H. K. Bisoyi, J.-Q. Jin, C.-L. Yuan, Z. Liu, D. Shen, Y.-Q. Lu, Z.-G. Zheng, W. Zhang, Q. Li, *Adv. Mater.* **2018**, *30*, 1800237.
229. F. Castles, F. V. Day, S. M. Morris, D. H. Ko, D. J. Gardiner, M. M. Qasim, S. Nosheen, P. J. Hands, S. S. Choi, R. H. Friend, H. J. Coles, *Nat. Mater.* **2012**, *11*, 599.
230. F. Castles, S. M. Morris, J. M. Hung, M. M. Qasim, A. D. Wright, S. Nosheen, S. S. Choi, B. I. Outram, S. J. Elston, C. Burgess, L. Hill, T. D. Wilkinson, H. J. Coles, *Nat. Mater.* **2014**, *13*, 817.
231. K. G. Gutierrez-Cuevas, L. Wang, Z.-G. Zheng, H. K. Bisoyi, G. Li, L.-S. Tan, R. A. Vaia, Q. Li, *Angew. Chem. Int. Ed.* **2016**, *55*, 13090.
232. S. H. Jung, J. Jeon, H. Kim, J. Jaworski, J. H. Jung, *J. Am. Chem. Soc.* **2014**, *136*, 6446.
233. P. Szustakiewicz, N. Kowalska, D. Grzelak, T. Narushima, M. Gora, M. Baginski, D. Pociecha, H. Okamoto, L. M. Liz-Marzan, W. Lewandowski, *ACS Nano* **2020**, *14*, 12918.
234. Y. Xu, X. Wang, W. L. Zhang, F. Lv, S. Guo, *Chem. Soc. Rev.* **2018**, *47*, 586.
235. H. Al-Bustami, B. P. Bloom, A. Ziv, S. Goldring, S. Yochelis, R. Naaman, D. H. Waldeck, Y. Paltiel, *Nano Lett.* **2020**, *20*, 8675.
236. R. Xiong, S. Yu, M. J. Smith, J. Zhou, M. Krecker, L. Zhang, D. Nepal, T. J. Bunning, V. V. Tsukruk, *ACS Nano* **2019**, *13*, 9074.
237. N. Suzuki, Y. Wang, P. Elvati, Z. B. Qu, K. Kim, S. Jiang, E. Baumeister, J. Lee, B. Yeom, J. H. Bahng, J. Lee, A. Violi, N. A. Kotov, *ACS Nano* **2016**, *10*, 1744.
238. T.-D. Nguyen, W. Y. Hamad, M. J. MacLachlan, *Adv. Funct. Mater.* **2014**, *24*, 777.
239. R. Kumar, K. K. Raina, *Liq. Cryst.* **2016**, *43*, 994.
240. Z. Li, L. Wang, Y. Li, Y. Feng, W. Feng, *Mater. Chem. Front.* **2019**, *3*, 2571.
241. H. Zheng, B. Ju, X. Wang, W. Wang, M. Li, Z. Tang, S. X.-A. Zhang, Y. Xu, *Adv. Opt. Mater.* **2018**, *6*, 1801246.
242. Z. Li, L. Wang, Y. Li, Y. Feng, W. Feng, *Compos. Sci. Technol.* **2019**, *179*, 10.
243. F. Li, Y. Li, X. Yang, X. Han, Y. Jiao, T. Wei, D. Yang, H. Xu, G. Nie, *Angew. Chem. Int. Ed.* **2018**, *57*, 2377.
244. F. Li, S. Li, X. Guo, Y. Dong, C. Yao, Y. Liu, Y. Song, X. Tan, L. Gao, D. Yang, *Angew. Chem. Int. Ed.* **2020**, *59*, 11087.
245. S. Kang, G. M. Biesold, H. Lee, D. Bukharina, Z. Lin, V. V. Tsukruk, *Adv. Funct. Mater.* **2021**, *31*, 2104596.
246. A. Doring, E. Ushakova, A. L. Rogach, *Light Sci. Appl.* **2022**, *11*, 75.
247. V. Kuznetsova, Y. Gromova, M. Martinez-Carmona, F. Purcell-Milton, E. Ushakova, S. Cherevkov, V. Maslov, Y. K. Gun'ko, *Nanophotonics* **2020**, *10*, 797.
248. A. Bobrovsky, K. Mochalov, V. Oleinikov, A. Sukhanova, A. Prudnikau, M. Artemyev, V. Shibaev, I. Nabiev, *Adv. Mater.* **2012**, *24*, 6216.
249. B. Zhang, J. Schmidtke, H.-S. Kitzerow, *Adv. Opt. Mater.* **2019**, *7*, 1801766.
250. T. P. Fraccia, G. P. Smith, G. Zanchetta, E. Paraboschi, Y. Yi, D. M. Walba, G. Dieci, N. A. Clark, T. Bellini, *Nat. Commun.* **2015**, *6*, 6424.
251. M. Giese, L. K. Blusch, M. K. Khan, M. J. MacLachlan, *Angew. Chem. Int. Ed.* **2015**, *54*, 2888.
252. A. V. P. Silvestrini, A. L. Caron, J. Viegas, F. G. Praca, M. Bentley, *Expert Opin. Drug Deliv.* **2020**, *17*, 1781.
253. Y. Habibi, L. A. Lucia, O. J. Rojas, *Chem. Rev.* **2009**, *110*, 3479.
254. O. Kose, A. Tran, L. Lewis, W. Y. Hamad, M. J. MacLachlan, *Nat. Commun.* **2019**, *10*, 510.
255. D. Klemm, B. Heublein, H. P. Fink, A. Bohn, *Angew. Chem. Int. Ed.* **2005**, *44*, 3358.
256. C. E. Boott, A. Tran, W. Y. Hamad, M. J. MacLachlan, *Angew. Chem. Int. Ed.* **2020**, *59*, 226.
257. R. Kadar, S. Spirk, T. Nypelo, *ACS Nano* **2021**, *15*, 7931.
258. Y. Cao, W. Y. Hamad, M. J. MacLachlan, *Adv. Opt. Mater.* **2018**, *6*, 1800412.
259. X. Wei, T. Lin, M. Duan, H. Du, X. Yin, *Bioresources* **2021**, *16*, 2116.
260. J. A. De La Cruz, Q. Liu, B. Senyuk, A. W. Frazier, K. Peddireddy, I. I. Smalyukh, *ACS Photonics* **2018**, *5*, 2468.
261. S. Zhao, Y. Yu, B. Zhang, P. Feng, C. Dang, M. Li, L. Zhao, L. Gao, *ACS Appl. Mater. Interfaces* **2021**, *13*, 59132.
262. B. A. San Jose, J. Yan, K. Akagi, *Angew. Chem. Int. Ed.* **2014**, *53*, 10641.
263. *Nanoscience with Liquid Crystals* (Ed: Q. Li), Springer, Heidelberg, Germany **2014**.
264. Y. Chen, P. Lu, Z. Li, Y. Yuan, H. Zhang, *Polym. Chem.* **2021**, *12*, 2572.
265. Y. Chen, P. Lu, Y. Yuan, H. Zhang, *J. Mater. Chem. C* **2020**, *8*, 13632.
266. S. Fukao, M. Fujiki, *Macromolecules* **2009**, *42*, 8062.
267. J. Guo, H. Cao, J. Wei, D. Zhang, F. Liu, G. Pan, D. Zhao, W. He, H. Yang, *Appl. Phys. Lett.* **2008**, *93*, 201901.
268. C. He, Z. Feng, S. Shan, M. Wang, X. Chen, G. Zou, *Nat. Commun.* **2020**, *11*, 1188.
269. C. Kulkarni, S. C. J. Meskers, A. R. A. Palmans, E. W. Meijer, *Macromolecules* **2018**, *51*, 5883.
270. M.-C. Li, N. Ousaka, H. F. Wang, E. Yashima, R. M. Ho, *ACS Macro Lett.* **2017**, *6*, 980.

271. K. Watanabe, I. Osaka, S. Yorozuya, K. Akagi, *Chem. Mater.* **2012**, *24*, 1011.
272. Y. Yang, R. C. da Costa, D. M. Smilgies, A. J. Campbell, M. J. Fuchter, *Adv. Mater.* **2013**, *25*, 2624.
273. Y. Zhao, L. Zhang, Z. He, G. Chen, D. Wang, H. Zhang, H. Yang, *Liq. Cryst.* **2015**, *42*, 1120.
274. Y. Chen, Z. Xu, W. Hu, X. Li, Y. Cheng, Y. Quan, *Macromol. Rapid Commun.* **2021**, *42*, e2000548.
275. J. He, K. Bian, N. Li, G. Piao, *J. Mater. Chem. C* **2019**, *7*, 9278.
276. A. Satrijo, S. C. J. Meskers, T. M. Swager, *J. Am. Chem. Soc.* **2006**, *128*, 9030.
277. Q. Liu, Q. Xia, S. Wang, B. S. Li, B. Z. Tang, *J. Mater. Chem. C* **2018**, *6*, 4807.
278. H. Maeda, Y. Bando, *Pure Appl. Chem.* **2013**, *85*, 1967.
279. K. Watanabe, K. Akagi, *Sci. Technol. Adv. Mater.* **2014**, *15*, 044203.
280. L. Yang, Y. Zhang, X. Zhang, N. Li, Y. Quan, Y. Cheng, *Chem. Commun.* **2018**, *54*, 9663.
281. B. Zhao, K. Pan, J. Deng, *Macromolecules* **2018**, *51*, 7104.
282. B. Zhao, K. Pan, J. Deng, *Macromolecules* **2018**, *52*, 376.
283. S.-K. Ahn, M. Gopinadhan, P. Deshmukh, R. K. Lakhman, C. O. Osuji, R. M. Kasi, *Soft Matter* **2012**, *8*, 3185.
284. X.-F. Chen, Z. Shen, X.-H. Wan, X.-H. Fan, E.-Q. Chen, Y. Ma, Q.-F. Zhou, *Chem. Soc. Rev.* **2010**, *39*, 3072.
285. M. A. Farooq, W. Wei, H. Xiong, *Langmuir* **2020**, *36*, 3072.
286. J. W. Goodby, A. J. Slaney, C. J. Booth, I. Nishiyama, J. D. Vuijk, P. Styring, K. J. Toyne, *Mol. Cryst. Liq. Cryst. Sci. Technol.* **2006**, *243*, 231.
287. M. Oda, H.-G. Nothofer, G. Lieser, U. Scherf, S. C. J. Meskers, D. Neher, *Adv. Mater.* **2000**, *12*, 5.
288. J. Yan, F. Ota, B. A. San Jose, K. Akagi, *Adv. Funct. Mater.* **2017**, *27*, 1604529.
289. A. Juan, H. Sun, J. Qiao, J. Guo, *Chem. Commun.* **2020**, *56*, 13649.
290. F. Song, Z. Xu, Q. Zhang, Z. Zhao, H. Zhang, W. Zhao, Z. Qiu, C. Qi, H. Zhang, H. H. Y. Sung, I. D. Williams, J. W. Y. Lam, Z. Zhao, A. Qin, D. Ma, B. Z. Tang, *Adv. Funct. Mater.* **2018**, *28*, 1800051.
291. N. Zhao, W. Gao, M. Zhang, J. Yang, X. Zheng, Y. Li, R. Cui, W. Yin, N. Li, *Mater. Chem. Front.* **2019**, *3*, 1613.
292. B. Xu, Z. Song, M. Zhang, Q. Zhang, L. Jiang, C. Xu, L. Zhong, C. Su, Q. Ban, C. Liu, F. Sun, Y. Zhang, Z. Chi, Z. Zhao, G. Shi, *Chem. Sci.* **2021**, *12*, 15556.
293. K. Akagi, T. Yamashita, K. Horie, M. Goh, M. Yamamoto, *Adv. Mater.* **2020**, *32*, e1906665.
294. S. Matsushita, M. Kyotani, K. Akagi, *J. Am. Chem. Soc.* **2011**, *133*, 17977.
295. Y. Cao, P.-X. Wang, F. D'Acierno, W. Y. Hamad, C. A. Michal, M. J. MacLachlan, *Adv. Mater.* **2020**, *32*, e1907376.
296. M. C. Heffern, L. M. Matosziuk, T. J. Meade, *Chem. Rev.* **2014**, *114*, 4496.
297. H. Maeda, Y. Bando, K. Shimomura, I. Yamada, M. Naito, K. Nobusawa, H. Tsumatori, T. Kawai, *J. Am. Chem. Soc.* **2011**, *133*, 9266.
298. F. Zinna, U. Giovanella, L. Di Bari, *Adv. Mater.* **2015**, *27*, 1791.

AUTHOR BIOGRAPHIES

Jiao Liu received her Ph.D. degree in Advanced Materials and Liquid Crystal Institute (AMLCI) at Kent State University in 2022. She is currently an assistant professor at Nanjing University of Posts and Telecommunications. Her research focuses on circularly polarized luminescent liquid crystal materials, liquid crystal elastomer, and stimuli-responsive soft matter.

Zhen-Peng Song is currently a Ph.D. student in Nanjing University of Posts and Telecommunications. His research mainly focuses on circularly polarized luminescent liquid crystal materials, liquid crystal elastomer, and the stimuli-responsive soft matter.

Lu-Yao Sun is currently a Ph.D. student in Nanjing University of Posts and Telecommunications. Her research mainly focuses on the electro-optical effects of liquid crystal and the stimuli-responsive soft matter.

Bing-Xiang Li received his Ph.D. degree in Chemical Physics from Advanced Materials and Liquid Crystal Institute at Kent State University in 2019. He is currently a professor at Nanjing University of Posts and Telecommunications. His current research spans from liquid crystals, stimuli-responsive soft matter, active matter, to biological physics.

Yan-Qing Lu received both his B.S. and Ph.D. degrees from Nanjing University, China, in 1991 and 1996, respectively. He has 5 years of experience in telecom industries in the United States and China. He is currently a Changjiang Distinguished Professor at Nanjing University and a Fellow of the Optical Society of America and Chinese Optical Society. His research interests include liquid crystal photonics, fiber optics, and nonlinear optics.

Quan Li is Distinguished Chair Professor and Director of Institute of Advanced Materials at Southeast University. He held appointments in USA, Germany, and France. Li received his Ph.D. from Chinese Academy of Sciences in Shanghai, where he was promoted to a youngest Full Professor in February 1998. He is a Fellow of the Royal Society of Chemistry. He has been elected as a member of the European Academy of Sciences and the European Academy of Sciences and Arts.

He has also honored as Professor and Chair Professor at several universities. His current research interest spans from stimuli-responsive smart soft matter, advanced photonics, and optoelectronic materials for energy harvesting and energy saving to functional biocompatible materials and nanoparticles to nanoengineering and device fabrication.

How to cite this article: J. Liu, Z.-P. Song, L.-Y. Sun, B.-X. Li, Y.-Q. Lu, Q. Li, *Responsive Materials* **2023**, e20230005. https://doi.org/10.1002/rpm.20230005